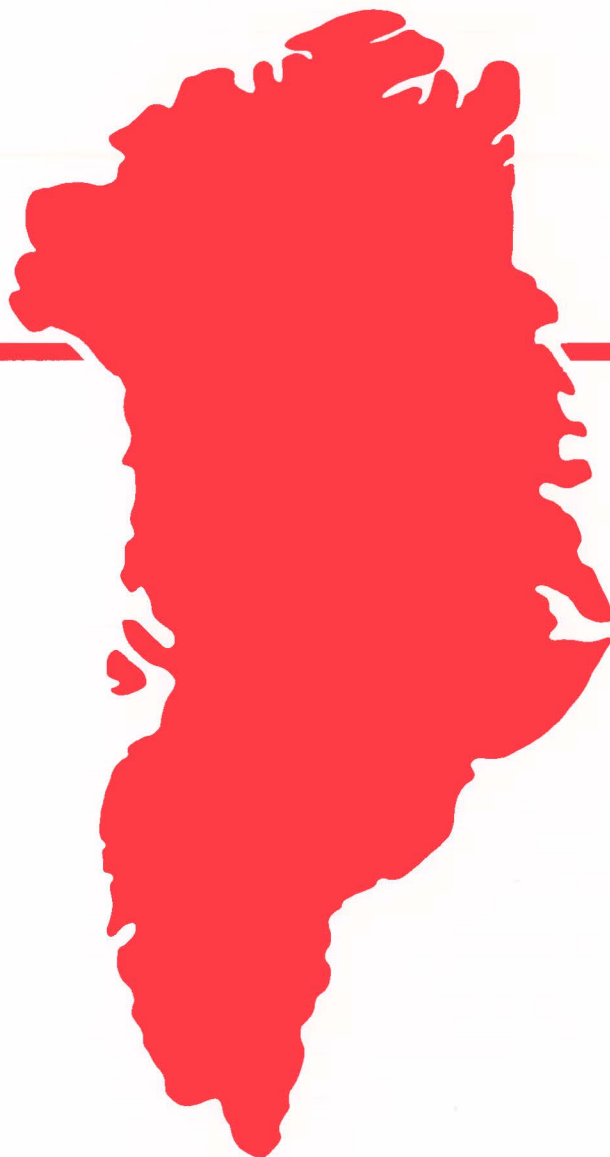


Reconnaissance geochemical exploration of map sheet
68 V 2 (67°55' to 68°45'N, 50°15' to 52°45'W),
West Greenland

Agnete Steenfelt, Else Dam
and Jens Peter Nielsen



Open File Series 92/7

July 1992



GRØNLANDS GEOLOGISKE UNDERSØGELSE
Ujarassioqut Kalaallit Nunaanni Misissuisoqarfiat
GEOLOGICAL SURVEY OF GREENLAND

GRØNLANDS GEOLOGISKE UNDERSØGELSE

Ujarassioqarfiat Kalaallit Nunaanni Misissuisoqarfiat

GEOLOGICAL SURVEY OF GREENLAND

The Geological Survey of Greenland (GGU) is a research institute affiliated to the Mineral Resources Administration for Greenland (MRA) within the Danish Ministry of Energy. As with all other activities involving the non-living resources in Greenland, GGU's investigations are carried out within the framework of the policies decided jointly by the Greenland Home Rule Authority and the Danish State.

Open File Series

The Open File Series consists of unedited reports and maps that are made available quickly in limited numbers to the public. They are a non-permanent form of publication that may be cited as sources of information. Certain reports may be replaced later by edited versions.

Citation form

Open File Series Grønlands Geologiske Undersøgelse

conveniently abbreviated to:

Open File Ser. Grønlands geol. Unders.

GGU's Open File Series består af uredigerede rapporter og kort, som publiceres hurtigt og i et begrænset antal. Disse publikationer er midlertidige og kan anvendes som kildemateriale. Visse af rapporterne vil evt. senere blive erstattet af redigerede udgaver.

ISSN 0903-7322

GRØNLANDS GEOLOGISKE UNDERSØGELSE

Open File 92/7

Reconnaissance geochemical exploration of map sheet 68 V 2
(67°55' to 68°45' N, 50°15' to 52°45' W), West Greenland

Agnete Steenfelt, Else Dam and Jens Peter Nielsen

July 1992

Abstract

The map sheet 68 V 2 has been covered by samples of stream sediment and water at a density of 1 sample site per c. 25 km² as part of the geochemical mapping programme of the Geological Survey of Greenland. The < 0.1 mm fraction of the sediment samples were analysed by X-ray fluorescence and instrumental neutron activation techniques and results are reported for 34 major and trace elements. The conductivity and fluoride content of the water samples were determined.

The results show that this part of the Archaean Laurentian shield which has been reworked during the Proterozoic has the geochemical signature of upper crust in agreement with common occurrences of supracrustal rocks in a basement dominated by infracrustal gneisses.

The economic potential is primarily associated with the supracrustal rock sequences and the anomaly patterns indicate mineralisation involving Au, As, Sb, Ba, Cu, Zn, U, and F in zones where hydrothermal activity related to either intrusion of late granites and pegmatites or to intense shearing has affected the supracrustals.

Introduction

The exploration carried out in map sheet 68 V 2 is part of the Geological Survey of Greenland's geochemical mapping programme based on drainage samples. The purpose of this programme is to provide reconnaissance geochemical data which may be used together with geophysical and geological information to outline provinces or zones with potential for mineral resources.

Samples were collected during the period 6th to 16th of July 1991 by J.P. Nielsen and E. Dam who were based in Qasigiannuguit (Christianshåb) and used a Bell 206 (Jet Ranger) helicopter for transportation.

Preliminary results concerning Au, As, and Sb were reported earlier this year in a regional evaluation of the gold potential of the Disko Bugt region (Steenfelt 1992). The map sheet 67 V 2, to the south of the present, was geochemically mapped and reported by Steenfelt and Dam (1991).

Administratively the surveyed area belongs to the communities of Qasigiannuguit, Aasiaat (Egedesminde) and Kangaatsiaq.

Geology

The survey area lies within the Nagssugtoqidian mobile belt of the Precambrian Laurentian shield (Escher et al., 1976; Korstgaard et al., 1969). The belt consists mainly of Archaean basement (gneiss with subordinate supracrustal sequences) which was reworked during the Proterozoic c. 1850 Ma ago (Fig. 1). In the fjord zone south of Arfersiorfik some units of calc-alkaline volcanic and plutonic rocks have been shown to be of Proterozoic juvenile origin (Kalsbeek et al., 1987); Proterozoic metasediments also occur.

Most of the Nagssugtoqidian (Proterozoic) deformation and magma generation is presently believed to be related to a collision between two Archaean continents about 1850 Ma ago (Kalsbeek et al., 1987; Bridgwater et al., 1990). However, geological field work has been very limited in the Nagssugtoqidian belt since the recognition of the Proterozoic age and juvenile origin of some of the rocks, and the exact character and location of a suture has not yet been established.

The coastal section of this region and the fjord zones was first mapped geologically by Noe-Nygaard & Ramberg (1961) and later at 1:250 000 by Henderson (1969) except for the southwesternmost part which was covered at 1:100 000 (Olesen, 1984).

The Archaean basement gneisses are mainly granodioritic in composition and in amphibolite facies except in the south-west where granulite facies rocks prevail, see Fig. 1 and 2. The enclaves of supracrustal rocks comprise sequences of semi-pelitic metasediments and marble as well as of basic volcanic rocks (amphibolites). Mineral assemblages in the metasediments and amphibolites indicate intermediate to upper amphibolite facies conditions (sillimanite, staurolite, garnet).

Henderson (1969) recognises at least three phases of deformation: an early system of tight folds which have been overprinted by the main deformation represented by upright to steeply inclined folds with axial planes trending between NE and E-W. A late, less pronounced fold phase appears to have NW-trending axial planes. In the Nagssugtoqidian the most conspicuous structural features are a number of ENE trending straight belts separating areas where the earlier large-scale fold structures are preserved (Henderson, 1969; Escher et al., 1976; see Fig. 1). Pronounced shear movements have been described by Sørensen (1983) in the Nordre Strømfjord shear zone (NSSZ) which transects the southernmost part of the survey area (Fig. 2). A sinistral offset of 115 km was estimated by Sørensen (1983).

The latest shear movements are Proterozoic as they affect the Arfersiorfik quartz diorite (1920 Ma of age, Kalsbeek et al., 1987), and so are some large open folds which involve Proterozoic supracrustals south of the NSSZ.

So far Proterozoic ages have only been obtained in the southernmost part of the survey area, south of the NSSZ (Kalsbeek et al., 1987), and both gneisses and supracrustal rocks in the Egedesminde district have yielded Archaean ages (Kalsbeek et al., 1987; Kalsbeek, pers. comm.). Thus the extent and degree of Archaean relative to Proterozoic deformation in the area north of NSSZ still has to be established.

The survey area contains Fe-Cu-Zn sulphide mineralisation at Lersletten (Fig. 2) which was found and investigated by Kryolitselskabet Øresund A/S in the 1960'es (Vaasjoki, 1965; Nielsen, 1976). The sulphides, comprising pyrrhotite and pyrite with minor chalcopyrite and sphalerite, are associated with a folded supracrustal sequence (mica and sillimanite schists, amphibolite and subordinate marble) cut by pegmatitic granites. A little molybdenite and arsenopyrite were also reported. The mineralisation is believed to have formed from syngenetic sedimentary sulphide deposits which were remobilised during the intrusion of granites and related pegmatites. The nearest larger granite stock is shown in Fig. 2, south west of the sulphide mineralisation. The granite and pegmatites

are later than the main deformation which affected the supracrustals, but the pegmatites themselves also show signs of deformation. The iron ore reserves are estimated at 3.5 million tons of probable ore and about 12 million of possible ore at a grade of 30-35 % Fe with additional Cu up to 0.5 % and Zn at about 2% (Nielsen, 1976).

Physiography

The relief of the surveyed area is moderate with elevations mainly varying between 100 and 600 m above sea level, except in the central western part where Holocene marine deposits uplifted to c. 100 m above present sea level constitute a large plain. Outside the plain the drainage pattern is fairly well developed but most of the streams are small and the rate of erosion is low except when streams are draining ice/snow fields. The streams are generally running from May to September, although those sustained only by melting snow usually dry up during July.

The bedrock exposure is generally good except in valleys and on gentle slopes where the surface is covered by talus and vegetation (herbs, grass, low scrubs).

Sampling

Eleven working days and 28 helicopter flying-hours were spent during the sampling of 259 sites distributed over 6000 square km. On average 25 samples were collected per day at a density of 1 site per 23 square km; 6 flying minutes were spent per sampling site, which is equal to 16 flying seconds per square km.

The sample sites were selected and marked on air photos prior to the sampling using criteria such as even distribution of the sites, a reasonable size of upstream drainage area, and a reasonable slope dip.

At each station c. 500 g of stream sediment was collected in a paper bag and 100 ml of stream water in a polyethylene bottle. In addition the radioactivity (total gamma-radiation) was measured on the surface of outcrops or stream boulders using a scintillometer (Table 1). To increase the representativity each stream sediment sample was composed of subsamples from 5 to 10 different sites of sand and silt deposits in the stream bed or banks. Duplicate samples of both sediment and water were collected at 24 sites which corresponds to 9 % of the sites.

Sample preparation and analysis

Sediment. The sample bags were air/sun-dried at the base-camp in Qasigiannuguit and then sent by ship to GGU, Copenhagen. Here the samples were further dried at 65° C and sieved into three grain size fractions using sieve apertures of 1 mm and 0.1 mm. The coarse fraction was discarded, the medium fraction archived and the fine fraction used for analysis. Samples were analysed at GGU by X-ray fluorescence and atomic absorption methods for major and some trace elements and at Activation Laboratories Ltd., Canada, by instrumental neutron activation analysis (INAA) for more trace elements, see Table 2.

Water. After collection the water samples (unfiltered and unacidified) were left at base camp for 24 hours to allow settling of eventual suspended matter and to acquire the same (room) temperature. Then the conductivity and fluoride concentration were measured (Table 1).

Data presentation

The analytical results are shown in this report as element distribution maps at the scale of 1:1 000 000 together with summary statistical parameters and histograms of the frequency distribution for each element (Fig. 3 to 40). Elements with insignificant concentrations are not included. In cases where an element has been determined by both X-ray fluorescence and instrumental neutron activation methods only one of the data sets is presented.

The geochemical maps include the analytical results of 48 samples collected in previous surveys to the north and south of the present in order to fill the space within the map frame.

The size of a dot is related to the element concentration in the sample as indicated below the histogram. In cases where the frequency distribution approximates log-normal the maximum dot size corresponds to the 98th percentile of the distribution. Otherwise the scaling of the dot-size is chosen so that variations in the geochemical background are displayed as clearly as possible. Maximum values are found in the statistical parameters in the figures, and values regarded as geochemical anomalies are shown on the anomaly map (Fig. 42).

Comments on the element distribution patterns

In general the element distribution patterns reflect the lithogeochemical variation over the survey area and high values for some elements can often be interpreted to indicate mineralisation. In the present map sheet the main contributors to the lithogeochemical variation are the gneisses, the supracrustal enclaves and the granite/pegmatite intrusions. However, the latter two rock groups, being small in dimension in relation to the sampling density, cannot be distinguished clearly as geochemical units. The response from these groups are seen as "noise" in the background patterns with clusters of high values for characteristic elements over the larger occurrences of these rocks.

The supracrustal rock group which has not been subdivided in Fig. 2, comprises basic metavolcanics ("amphibolites"), and metasediments including subordinate marble. Enclaves of these rocks occur frequently in the basement gneisses, also as abundant smaller units which cannot be shown on the simplified geological map of Fig. 2. The presence of amphibolites in the gneisses is reflected by scattered elevated values of Mg, Co, and Cu whereas the metasediments, having a gross chemical composition similar to the surrounding gneisses, are only reflected by higher concentrations of elements derived from mineralisation within the metasediments: Zn, Cu, As. The marble occurrences are too small to influence the element distribution patterns. The lithophile elements K and Rb are high over the occurrences of late granites and pegmatites showing that this generation of granite probably represents anatexis of a crustal source.

In Table 3 the medians for element concentrations over the whole of map sheet 68 V 2 are compared with average values for upper and lower crust according to Taylor and McLennan (1985). For most of the elements the terrain of 68 V 2 corresponds to upper crust which is in agreement with the predominance of granodioritic gneisses and the abundance of supracrustal rocks metamorphosed under amphibolite facies conditions.

The section of the Nagssuqtoqidian belt presented in this report is small which means that large scale geochemical distribution patterns defined by the reconnaissance geochemical mapping (Steenfelt, 1987; Steenfelt and Dam, 1991) cannot be properly recognised within 68 V 2. Consequently, further evaluation of the significance of the regional geochemical variation in relation to crustal structure should await the completion of the sampling of the entire Nagssuqtoqidian belt, which is expected to happen 1993.

Element distribution indicating mineralisation

In 68 V 2 the distribution patterns for high values of Au, As, Sb, Ba, Cu, and Zn are considered suggestive of mineralisation associated with supracrustal sequences and with the Nordre Strømfjord shear zone (NSSZ). Also F in stream water is known to be an indicator of hydrothermal activity (Steenfelt, 1987) and the high values of F and conductivity along the supracrustal rocks at Lersletten and the NSSZ, particularly in its eastern end, could well be indicative of a hydrothermal, possibly mineralising activity.

The unusually high values of U (up to 60 ppm) along the NSSZ indicate uranium mineralisation which could be associated with the hydrothermal activity indicated by the F anomalies, whereas the high U values in the northern part of 68 V 2 probably reflect uranium minerals in pegmatites. Pegmatites are common in the northern region (Henderson, 1969, and observations during the sampling) and blocks of pegmatites encountered at the stream sediment sampling sites were often found to be radioactive (compare Fig. 37).

Comparison with neighbouring areas

The geochemical maps are presented in the same format and scale as those covering the area to the south of 68 V 2 (67 V 2, Steenfelt and Dam, 1991), and there is a 10 latitude minutes overlap between the two so as to ease comparison. However, the scaling of the dot size is optimised for 68 V 2 and is not always the same as for the same element in 67 V 2. For all of the elements analysed with the Instrumental Neutron Activation method the analytical results are fully comparable between the two surveys, but for the elements Ni, Sr, V, and Zn, analysed with X-ray Fluorescence Spectrometry, the analytical results showed an analytical bias between the two surveys. In this presentation the values for Ni have been levelled arithmetically to be comparable with the 67 V 2 results, but for the other elements mentioned the levels are not directly comparable.

Supplementary investigations

In the course of the stream sediment programme samples were also collected to examine 1) the geochemical response from the Lersletten mineralisation in the surrounding soil, 2) the composition of some sulphide mineralised rocks and 3) the composition of the Quaternary marine clay of the lowlands (Fig. 2).

Soil results. Samples were collected in the neighbourhood of a conspicuous ridge exposure of rusty rocks which has been drilled by Kryolitselskabet Øresund A/S (KØ), see location Fig. 40, and sketch map in Fig. 41. At the top of the ridge weathering products form a loose, non-vegetated, rusty coloured soil, whereas the surrounding slopes are irregularly covered by 5 to 30 centimetres of soil supporting a low vegetation. At each locality c. 500 g soil was collected into a stream sediment sample bag from 4 different sites spaced over a few square metres. In vegetated sites the soil samples were taken below the humus layer, close to the underlying bedrock. The samples were dried, sieved and analysed in the same way as the stream sediment samples. Analytical results are shown in Table 4.

All of the samples contain As above the detection limit of 2 ppm which can be regarded as slightly anomalous. The samples of rusty soil immediately below the mineralised bedrock, sample no.'s 380057 - 380059, are enriched in Au and other elements typically associated with gold mineralisation: As, Sb, Mo, Se, and also show high V and Zn. Anomalous enrichment in Au, As, or Sb is also found in some of the more distal samples 380052, 380055 and 380060.

Half of the samples are enriched in Cu with highest values in 380050 and 380054. The soil chemistry thus confirms the Cu and Zn enrichment previously described (Vaasjoki, 1965) but also suggests a gold potential which warrants further investigation. The Cu and Zn anomalies are not very high and do not suggest any higher grades than previously assumed (Vaasjoki, 1965).

Rock samples. A considerable number of rust zones were observed from the air during the sampling, and a few of these were inspected on ground. Small amounts of graphite, pyrite and pyrrhotite were found in the limonite rich zones hosted by amphibolite or schist. Ten grab samples of rusty rock sequences from four localities were collected for analysis (Table 5 and Fig. 41).

Loc. 1 (Lersletten): The quartz vein is weakly Zn mineralised otherwise blank. The sulphide sample confirms the known Zn enrichment, and also shows the Au-As-Sb-Mo-Se association seen in the soil.

Loc. 2: This locality of sulphide mineralised mica schist resembles the Lersletten mineralisation and the samples also show the same chemical characteristics, i.e. increased concentrations of As, Sb, Zn, Mo, Se.

Loc. 3. The samples were collected from a prominent rust zone in the east west striking supracrustal enclave of amphibolite (s.l.) during a short helicopter ground stop. The mineralisation visited consists of less than one meter wide conformable sulphide rich bands also containing biotite-garnet rich horizons. Besides sulphide, sample 360825 consists of staurolite, diopside,

quartz and garnet, an assemblage which could be interpreted to represent metamorphosed iron rich siliceous sediments interleaved with the basaltic volcanic rocks. The mineralised samples 360824 and 360825 show the highest Au values and also contain detectable Se and fairly high Zn but they differ from the Lersletten samples in being devoid of As and Sb.

Loc. 4. This sequence of rusty rocks comprises amphibolite, graphitic quartzite and marble, but the analyses do not show any enrichment in ore metals other than Zn.

Marine clay. The marine deposits are light grey to bluish grey clay (in terms of grain size) occasionally containing a few mm to 2 cm thick seams of silt. Shells or other remnants from marine animals witness to the contact of the deposits with a marine environment. The clay was sampled at two different sites and two samples were collected from each site. The samples were treated and analysed in the same way as the stream sediments.

The samples of the clay deposits are fairly close in composition to each other and also to the stream sediment medians except for the elements marked with an asterisk in Table 6 which have higher concentrations in the clay. The gross chemical similarity implies that the clay is likely to be derived from the same kind of bedrock terrain as the stream sediments. The difference may be explained by assuming that the clay contains more biotite than the stream sediments. This is reasonable because by experience biotite as small flakes is usually carried away with the stream water and escapes deposition in normal stream beds (Kalsbeek, 1971). On the contrary, in a situation where the glaciofluvial silt and clay fraction is deposited in a large reservoir, lake or sea, the biotite flakes are expected to settle with the other particles. The calculation presented in Table 6 shows that a 10% addition of biotite to the median stream sediment composition almost obliterates the difference in chemistry. A biotite content would also account for the higher concentrations of Cr, Cu, Ni, Rb and Zn in the clay.

The higher concentration of Na in the clay is not accounted for by biotite addition, but is an obvious reflection of the marine environment. The chemistry together with the character of the deposits suggest that they represent glaciofluvial deposits which were submersed below sea water for a period of time and then later uplifted again. During the stay in the marine environment the sedimentary deposits were enriched in Na.

Interpretation of mineralisation indications

The location of the highest values for elements considered to be indicative of mineralisation is shown in Fig. 42. The anomalies appear to form clusters around two main geological settings which are considered favourable for mineralisation in this area: 1) The supracrustal sequences at Qasigiannguit, Ikamiut, Lersletten, Qoorsunnitsoq, "Loc. 3", and 2) the Nordre Strømfjord Shear Zone.

Qasigiannguit. The two Au anomalies are not associated with anomalously high values for other elements. They belong to a cluster of 14 Au containing samples derived from the supracrustal enclaves south east and east of Qasigiannguit (Steenfelt, 1992). The supracrustals are dominated by rusty metasediments and also contain a little marble (Henderson, 1969). The locality has not been studied on ground during the geochemical reconnaissance programme.

Ikamiut. The Archaean (Kalsbeek, pers. comm.) sequence of metasediments and metavolcanics has high As and Sb (and just detectable Au), as well as high Ba, Cu and Zn. The high Rb and U indicate granitic or granite pegmatitic influence within and west of the occurrence of supracrustals. The metal association is compatible with a Lersletten epigenetic type of mineralisation.

Lersletten. The ENE trending zone of supracrustals comprising the Lersletten Fe-Zn-Cu sulphide mineralisation (Le in Fig. 42) is characterised by Au, As, Sb, Cu, Zn anomalies in stream sediment and F in stream water. A cluster of high values for the same elements extends in a north-westerly direction from the granite stock in the western end of the Lersletten supracrustal zone. The element association and spatial distribution of the anomalies agree with previous assumptions (Vaasjoki, 1965) that the epigenetic mineralisation was generated by hydrothermal activity in connection with the intrusion of the granite. The analyses of the soil and rock samples from the mineralisation have a characteristic enrichment in Se and Mo (Se and Mo are normally below the detection limits) which are often associated with gold mineralisation (Boyle, 1979).

It is probably no coincidence that the anomalies at Lersletten align with U, Sb and F anomalies to the ENE (and a single Sb anomaly to WSW), as this direction, marked with a dashed line in Fig. 42, is the main structural trend in the region. A speculative interpretation is that the intrusion of acid magma as well as the associated hydrothermal activity follows a crustal lineament e.g. a shear or fracture zone. The recognition of such a lineament may be impeded by the deposits of marine clay which cover at least a part of its trend.

Qoorsunnitsoq. The small cluster of anomalies in Au, Sb, Cu, and Zn may be related to a mineralisation of the Lersletten type in the supracrustal rocks on this small island.

Loc. 3. This locality with indication of Au mineralisation appears to be different from in the Lersletten mineralisation in host rock, amphibolite instead of mica schist, and in element association, Au and Se but no high As, Sb or Zn.

Nordre Strømfjord shear zone. All the elements listed in Fig. 42 have anomalously high values within the shear zone. The spatial distribution suggests that possible mineralising activity is related to the shear movements, whereas the element association suggests that the metals are derived from the supracrustal sequences occurring within the shear zone.

Conclusion

The geochemical maps of 68 V 2 based on analysis of the <0.1 mm grain size fraction of stream sediment plus conductivity and fluoride determinations of stream water show clusters of high values for Au, As, Sb, Ba, Cu, Zn, U, and F which can be interpreted to indicate mineralisation in 1) assumed Archaean supracrustal sequences and 2) a large Proterozoic shear zone.

The lithology of the supracrustal sequences suggests that they were deposited in a platform or intracratonic type of setting. Seen on a regional scale the element distribution patterns related to the supracrustals display slightly elevated background values for Au, As, Cu, and Zn by comparison with neighbouring areas (Steenfelt and Dam, 1991; Steenfelt, 1992). This may be interpreted to indicate primary syngenetic enrichment in these elements in the volcano-sedimentary environment. The high values of F in water occurring together with anomalously high values for the elements mentioned above is interpreted as an indication of mineralisation caused by hydrothermal activity in connection with intrusion of granitic magma in the northern part of map sheet 68 V 2 and in connection with major shear movements in the southern part.

Acknowledgment. The sampling benefitted greatly from the skill and keen cooperation of the GLACE helicopter pilot Urs Stoller.

References

- Bridgwater, D., Austrheim, H., Hansen, B. T., Mengel, F., Pedersen, S. & Winter, J. 1990: The Proterozoic Nagssugtoqidian mobile belt of southeast Greenland: A link between the eastern Canada and Baltic shields. Geosci. Can. 17, 305-310.
- Boyle, R. W. 1979: The geochemistry of gold and its deposits (together with a chapter on geochemical prospecting for the element). Bull. Geol. Surv. Can. 280, 584 pp.
- Deer, W. A., Howie, R. A. & Zussman, J. 1966: An introduction to the rock forming minerals. London: Longman.
- Escher, A. 1971: Geological map of Greenland. 1:500 000 sheet 3, Søndre Strømfjord - Nūgssuaq. Copenhagen: Geol. Surv. Greenland.
- Escher, A., Sørensen, K. & Zeck, H. P. 1976: Nagssugtoqidian mobile belt in West Greenland. In Escher, A. & Watt, W. S. (ed.) Geology of Greenland, 77-95. Copenhagen: Geol. Surv. Greenland.
- Henderson, G. 1969: The Precambrian rocks of the Egedesminde-Christianshåb area, West Greenland. Rapp. Grønlands geol. Unders. 23, 37 pp.
- Kalsbeek, F. 1971: The composition of sands from the Fiskenæsset region, South West Greenland, and its bearing on the bedrock geology of the area. Rapp. Grønlands geol. Unders. 40, 12 pp.
- Kalsbeek, F., Pidgeon, R. T. & Taylor, P. 1987: Nagssugtoqidian mobile belt of West Greenland: a cryptic suture between two Archaean continents - chemical and isotopic evidence. Earth Planet. Sci. Lett. 85, 365-385.
- Korstgård, J. A. (ed.) 1979: Nagssugtoqidian geology. Rapp. Grønlands geol. Unders. 89. 146 pp.
- Nielsen, B. L. 1976: Economic minerals. In Escher, A. & Watt, W. S. (ed.) Geology of Greenland, 461-486. Copenhagen: Geol. Surv. Greenland.
- Noe-Nygaard, A. & Ramberg, H. 1961: Geological reconnaissance map of the country between latitudes 69°N and 63°45' N, West Greenland. Meddr Grønland, 123 (5), 1 map, 9pp.
- Olesen, N. Ø. 1984: Geologisk kort over Grønland 1:100 000, Agto 67 V.1 Nord. Copenhagen: Geol. Surv. Greenland.
- Steenfelt, A. 1992: Gold, arsenic and antimony in stream sediment related to supracrustal units between Arfersiorfik and Qarajaq Isfjord (68°N to 70°30'N), West Greenland. Open File Ser. Grønlands geol. Unders. 92/4, 11 pp, 5 figs, 2 tables.

- Steenfelt, A. & Dam, E. 1991: Reconnaissance geochemical exploration of map sheet 67 V 2 (67° to 68°N, 49°30' to 52°W), West Greenland. Open File Ser. Grønlands geol. Unders. 91/8. 13 pp.- 42 figs.
- Sørensen, K. 1983: Growth and dynamics of the Nordre Strømfjord shear zone. J. Geophys. Res. 88, 3419-3437.
- Taylor, S. R. & McLennan, S. M. 1985: The Continental Crust: its Composition and Evolution. Oxford: Blackwell Scientific Publications, 312 pp.

Table 1. Instrumentation at the Geological Survey of Greenland

Field measurement of gamma-radiation: Saphymo-Srat SPP-2 scintillometer

Water samples:

Conductivity: Chemotest JK 8800

Fluoride concentration: Orion EA 920 pH/ion analyzer

Stream sediment samples:

Major and trace elements (see Table 2): Philips PW 1606 Multichannel X-ray
Fluorescence Spectrometer

Cu, Na₂O: Perkin Elmer 2280 Atomic Absorption Spectrometer

Table 2. Analytical detection limits.

Instrumental Neutron Activation Analysis (Activation Laboratories Ltd.)

Au	5.0 ppm	Ag	5.0 ppm	As	2.0 ppm	Ba	100.0 ppm
Br	1.0 ppm	Ca	1.0 %	Co	5.0 ppm	Cr	10.0 ppm
Cs	2.0 ppm	Fe	0.02 %	Hf	1.0 ppm	Hg	1.0 ppm
Ir	5.0 ppm	Mo	5.0 ppm	Na	500.0 ppm	Ni	50.0 ppm
Rb	30.0 ppm	Sb	0.2 ppm	Sc	0.1 ppm	Se	5.0 ppm
Sn	0.01 %	Sr	0.05 %	Ta	1.0 ppm	Th	0.5 ppm
U	0.05 ppm	W	4.0 ppm	Zn	50.0 ppm	La	1.0 ppm
Ce	3.0 ppm	Nd	5.0 ppm	Sm	0.1 ppm	Eu	0.2 ppm
Tb	0.5 ppm	Yb	0.05 ppm	Lu	0.05 ppm		

X-ray Fluorescence Spectrometry

	%		ppm
SiO ₂	0.034	V	5
TiO ₂	0.002	Cr	5
Al ₂ O ₃	0.004	Ni	2
Fe ₂ O ₃	0.0014	Zn	10
MnO	0.0013	Rb	2
MgO	0.023	Sr	1
CaO	0.002		
K ₂ O	0.0026		
P ₂ O ₅	0.004		

Atomic Absorption Spectrometry

Na ₂ O	0.05%
Cu	5 ppm

Table 3. Selected element concentrations in 68 V 2 compared with estimates for upper and lower crust by Taylor & McLennan (1985).

	SiO ₂	TiO ₂	Al ₂ O ₃	Fe ₂ O ₃	MnO	MgO	CaO	Na ₂ O	K ₂ O			
68 V 2 medians	65.0	0.45	13.8	4.4	0.08	1.8	3.9	3.3	1.6			
Upper crust	66.0	0.5	15.2	5.0	0.06	2.2	4.2	3.9	3.4			
Lower crust	54.4	1.0	16.1	11.8	0.17	6.3	8.5	2.8	0.34			
	Sc	V	Cr	Co	Ni	Cu	Zn	Rb	Sr	Ba	Th	U
68 V 2 medians	12	48	67	12	43	21	20	28	358	420	6	3
Upper crust	11	60	35	10	20	25	71	112	350	550	11	3
Lower crust	36	285	235	35	135	90	83	5	230	150	1	0.3
	La	Ce	Nd	Sm	Eu	Yb	Lu					
68 V 2 medians	32	59	27	4	1.10	1.9	0.27					
Upper crust	30	64	26	4.5	0.88	2.2	0.32					
Lower crust	11	23	13	3.2	1.17	2.2	0.29					

Table 4. Chemical composition of soil samples collected around the Lersletten prospect. Major elements, V, Ni, Zn and Cu X-ray fluorescence analysis by GGU. Au to U instrumental neutron activation analysis by Activation Laboratories Ltd.

GGU no.	SiO ₂ %	TiO ₂ %	Al ₂ O ₃ %	Fe ₂ O ₃ %	MnO %	MgO %	CaO %	Na ₂ O %	K ₂ O %	P ₂ O ₅ %	Vol %
380050	53.93	0.39	12.70	7.37	0.24	1.95	3.74	2.71	1.285	0.215	14.88
380051	59.23	0.50	11.14	13.31	0.07	1.84	3.32	2.73	1.444	0.123	6.13
380052	56.74	0.50	9.90	16.26	0.05	1.58	2.88	2.70	1.390	0.129	7.71
380053	65.88	0.41	14.44	5.27	0.07	1.83	3.90	3.42	1.680	0.135	2.82
380054	60.00	0.33	12.73	4.20	0.06	1.45	3.47	2.95	1.431	0.103	13.17
380055	61.05	0.39	13.35	4.73	0.08	1.86	4.25	3.17	1.393	0.146	9.39
380056	62.87	0.48	13.33	8.41	0.07	1.93	3.90	3.17	1.528	0.096	3.79
380057	52.54	0.67	10.23	18.20	0.07	1.93	3.34	2.83	1.288	0.099	8.75
380058	58.18	0.56	12.59	12.21	0.08	2.24	4.03	3.06	1.362	0.091	5.65
380059	50.08	0.86	10.44	21.04	0.07	2.19	3.38	2.74	1.206	0.116	7.95
380060	61.89	0.63	15.27	6.27	0.09	2.82	3.97	3.13	2.123	0.136	3.29
380061	63.58	0.56	12.43	8.29	0.08	2.21	4.00	3.01	1.475	0.104	3.56
380062	67.63	0.46	14.71	4.55	0.09	1.80	4.00	3.50	1.677	0.147	1.12
380063	63.20	0.44	13.80	5.00	0.08	1.82	3.58	3.16	1.595	0.126	6.51

GGU no.	Au ppb	As ppm	Sb ppm	Ba ppm	Co ppm	Cr ppm	Mo ppm	Se ppm	Th ppm	U ppm	V ppm	Ni ppm	Zn ppm	Cu ppm
380050	0	6	0.0	330	69	66	0	0	3.3	1.3	63	72	38	226
380051	0	7	0.0	400	11	100	0	0	4.0	1.1	70	55	26	94
380052	5	13	0.4	360	9	87	0	0	4.4	0.0	73	58	22	92
380053	0	6	0.0	450	12	71	0	0	3.4	0.9	51	58	19	59
380054	0	2	0.0	420	10	65	0	0	3.2	4.5	48	34	9	154
380055	0	3	0.2	400	14	69	0	0	3.3	1.3	47	43	18	53
380056	0	14	0.4	430	13	76	0	0	3.2	1.1	71	49	31	49
380057	5	32	1.3	340	6	78	16	5	2.5	1.1	160	45	99	64
380058	0	17	0.6	320	12	78	7	5	2.8	0.7	106	69	57	57
380059	9	28	1.8	390	8	91	25	8	2.8	0.7	208	55	83	86
380060	13	17	0.0	470	40	120	0	0	7.7	2.5	83	123	46	72
380061	7	9	0.0	390	10	86	0	0	3.9	1.2	96	64	33	32
380062	0	10	0.0	410	14	74	0	0	4.1	1.0	60	46	34	44
380063	0	18	0.0	440	17	88	0	0	4.2	2.2	54	49	18	26

Table 5. Element concentrations of grab samples from rusty rock sequences. Instrumental neutron activation analysis by Activation Laboratories Ltd.

GGU no.	Au ppb	As ppm	Ba ppm	Ca %	Co ppm	Cr ppm	Fe %	Mo ppm	Ni ppm	Rb ppm	Sb ppm	Se ppm	Th ppm	U ppm	Zn ppm
360807	40	52	400	0	66	33	38.70	79	270	0	7.6	12	0.6	17.0	1640
360811	0	0	0	0	0	20	0.25	0	0	0	0.0	0	0.0	0.0	104
360820	71	190	240	0	96	22	36.30	26	510	45	1.7	13	1.3	8.5	0
360821	0	30	1600	1	12	100	3.26	n.d.	0	110	0.5	0	7.8	5.1	127
360824	26	0	0	3	24	23	21.70	0	0	0	0.0	5	0.7	0.0	133
360825	269	0	0	4	20	26	20.40	0	0	0	0.0	7	0.0	1.1	120
360826	16	0	360	7	45	1100	7.95	0	180	0	0.6	0	5.4	0.0	149
360827	0	5	260	10	24	150	8.12	0	0	0	0.0	0	1.0	0.0	200
360828	0	0	0	26	0	0	0.65	0	0	0	0.0	0	0.0	0.0	0
360830	0	0	0	0	0	12	0.63	0	0	0	0.0	0	0.0	1.9	0

360807 massive pyrrhotite with sphalerite
 360811 quartz vein
 360820 massive sulphide
 360821 mica schist
 360824 sulphide rich layer in amphibolite
 360825 sulphide rich layer in amphibolite
 360826 amphibolitic host rock
 360827 amphibolite
 360828 carbonate
 360830 quartzite with graphite

Table 6. Chemical composition of Holocene marine "clay" compared with the composition of stream sediments. 68V2md = medians of stream sediments in 68 V 2. 68V2bt = 10% biotite added to median composition. Biotite = composition of biotite from a garnet-sillimanite-mica schist (taken from Deer et al., 1966). The asterisks mark elements which are significantly enriched in the "clay" relative to the stream sediments. Major elements and V to Sr X-ray fluorescence analysis by GGU. As to Yb instrumental neutron activation analysis by Activation Laboratories Ltd.

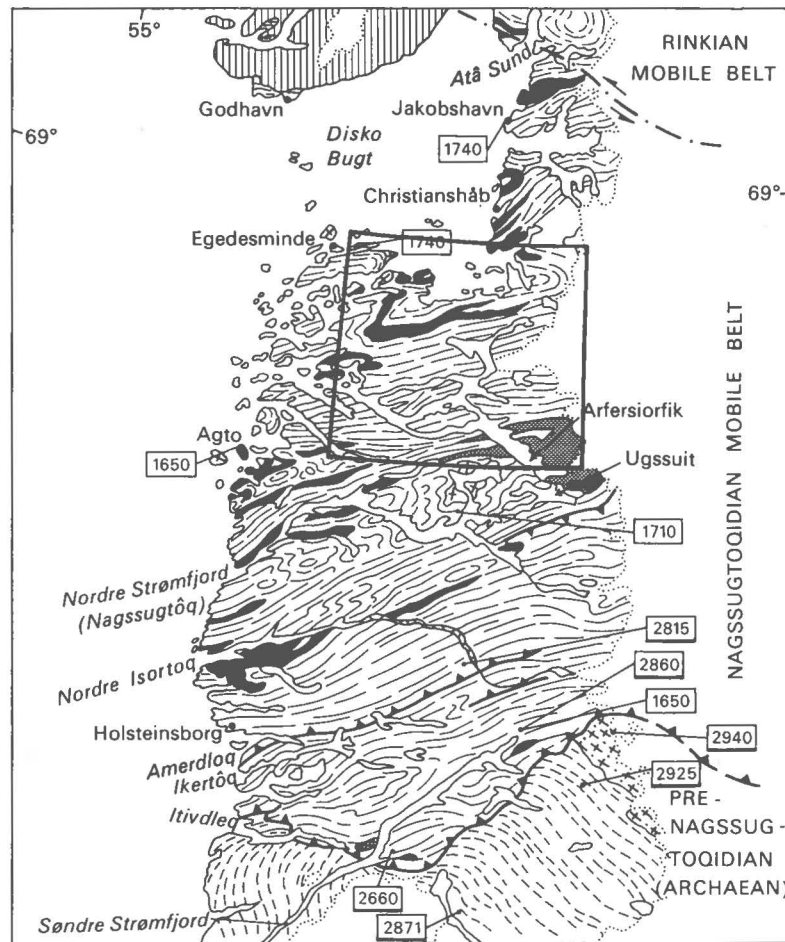
GGU no.	SiO ₂ %	TiO ₂ %	Al ₂ O ₃ %	Fe ₂ O ₃ %	MnO %	MgO %	CaO %	Na ₂ O %	K ₂ O %	P ₂ O ₅ %	Vol %
380152	63.06	0.68	15.58	5.63	0.08	3.04	3.85	3.88	2.626	0.156	1.21
380153	59.99	0.69	16.40	6.79	0.09	3.76	3.60	3.58	3.077	0.160	1.50
380289	65.91	0.44	14.87	4.73	0.07	2.44	3.98	3.96	2.229	0.150	0.93
380290	66.59	0.45	14.47	4.49	0.08	2.24	4.33	3.83	1.986	0.179	0.78
			*	*		*		*	*		
68V2md	65.0	0.45	13.8	4.4	0.08	1.8	3.9	3.3	1.6	0.16	4.8
68V2+bt	62.0	0.66	14.46	6.34	0.07	2.33	3.53	3.07	2.30	-	4.69
Biotite	35.03	2.56	20.38	23.77	0.02	7.11	0.17	0.96	8.62	n.d.	3.67

GGU no.	As ppm	Ba ppm	Co ppm	Cr ppm	Hf ppm	Sc ppm	Th ppm	U ppm	La ppm	Yb ppm
380152	3	520	15	85	4	13	6.8	0.9	32	1.40
380153	2	480	20	120	3	15	9.9	1.1	41	1.31
380289	0	450	12	82	6	12	5.7	1.2	24	1.58
380290	4	420	12	81	9	12	5.0	1.1	23	2.11
				*						
68V2md	0	420	12	67	10	12	6	3	32	1.87

GGU no.	V ppm	Ni ppm	Cu ppm	Zn ppm	Rb ppm	Sr ppm
380152	73	98	38	32	46	300
380153	83	85	51	69	95	285
380289	51	61	31	31	55	407
380290	38	47	26	22	47	412
		*	*	*	*	
68V2md	48	43	21	20	28	358

List of figures

- Fig. 1. Location of the survey area in the Nagssugtoqidian mobile belt. From Escher et al., 1976.
- Fig. 2. Simplified geological map of the survey area. After Escher (1971).
- Fig. 3. Geochemical map of 68 V.2: SiO_2 in stream sediment
- Fig. 4. TiO_2
- Fig. 5. Al_2O_3
- Fig. 6. Fe_2O_3
- Fig. 7. MnO
- Fig. 8. MgO
- Fig. 9. CaO
- Fig. 10. Na_2O
- Fig. 11. K_2O
- Fig. 12. P_2O_5
- Fig. 13. As
- Fig. 14. Au
- Fig. 15. Ba
- Fig. 16. Co
- Fig. 17. Cr
- Fig. 18. Cu
- Fig. 19. Hf
- Fig. 20. Ni
- Fig. 21. Rb
- Fig. 22. Sb
- Fig. 23. Sc
- Fig. 24. Sr
- Fig. 25. Th
- Fig. 26. U
- Fig. 27. V
- Fig. 28. Zn
- Fig. 29. La
- Fig. 30. Ce
- Fig. 31. Nd
- Fig. 32. Sm
- Fig. 33. Eu
- Fig. 34. Tb
- Fig. 35. Yb
- Fig. 36. Lu
- Fig. 37. Map of gamma-radiation within 68 V.2.
- Fig. 38. Geochemical map of 68 V.2: Conductivity of stream water.
- Fig. 39. Fluoride
- Fig. 40. Sketch map of location of soil samples at Lersletten.
- Fig. 41. Locality map of analysed soil, rock and clay samples.
- Fig. 42. Distribution map of geochemical anomalies.



-  Phanerozoic cover
- NAGSSUGTOQIDIAN**
-  Granites, mainly syn-kinematic
-  Quartz diorite
-  Supracrustal rocks
-  Gneisses
-  Anorthosite
- PRE-NAGSSUGTOQIDIAN**
-  Charnockites and syenites
-  Gneisses
-  Thrust
-  Wrench fault
-  1710 K/Ar age of biotites (m.y.)
-  2815 U/Pb age of zircons (m.y.)

Fig.1

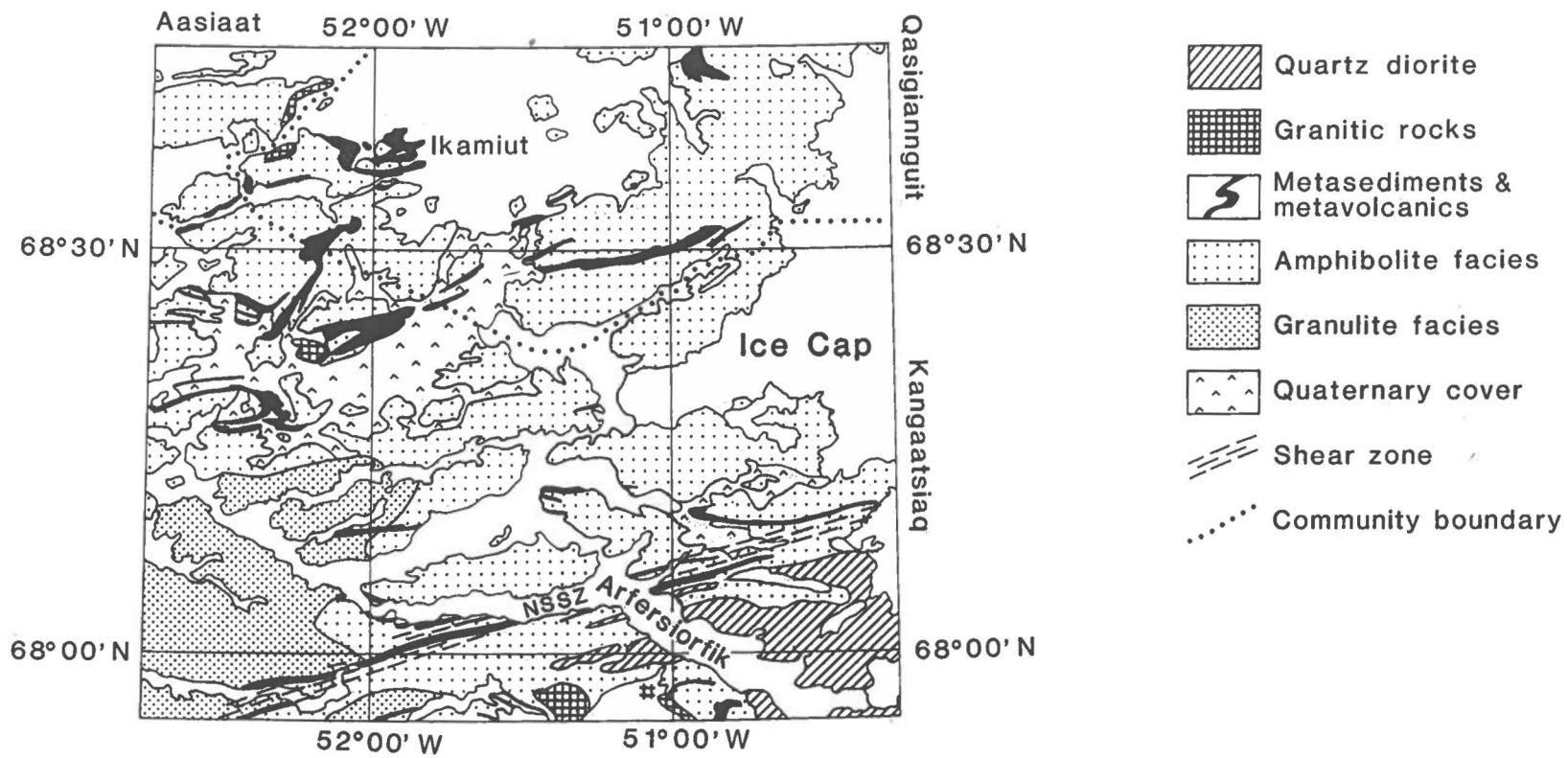
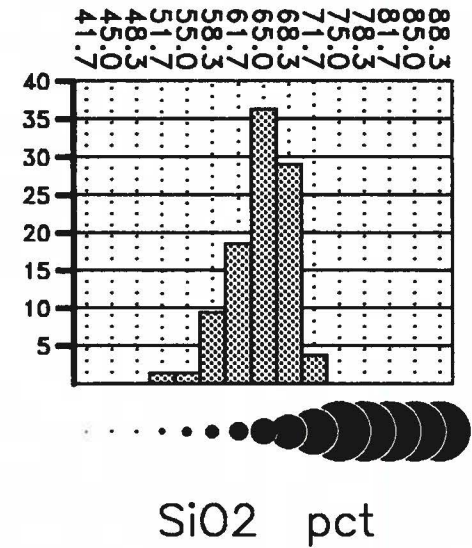
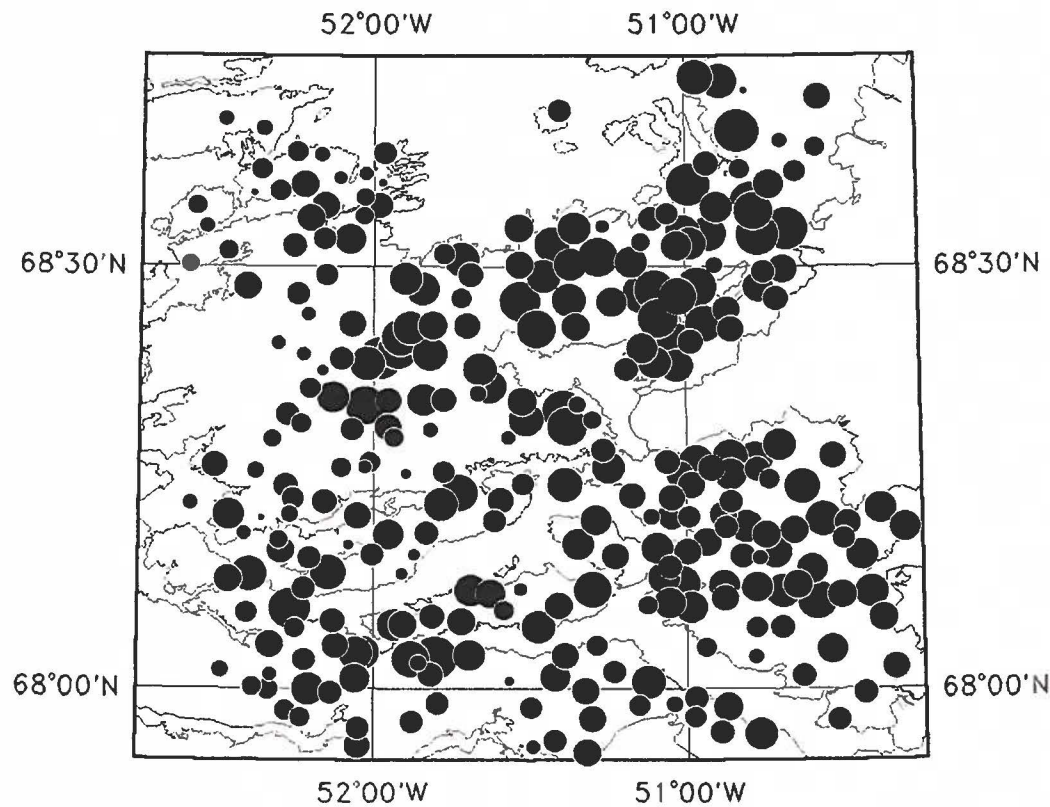


Fig. 2



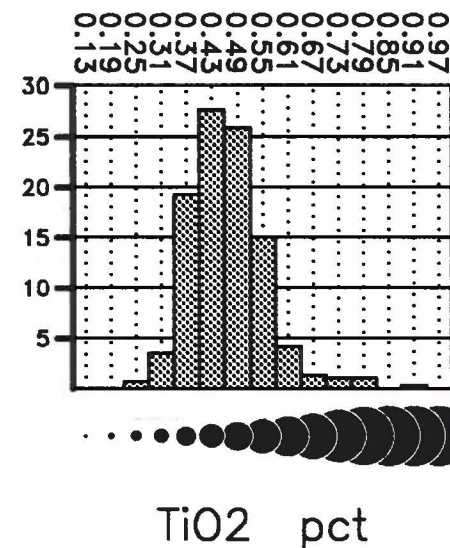
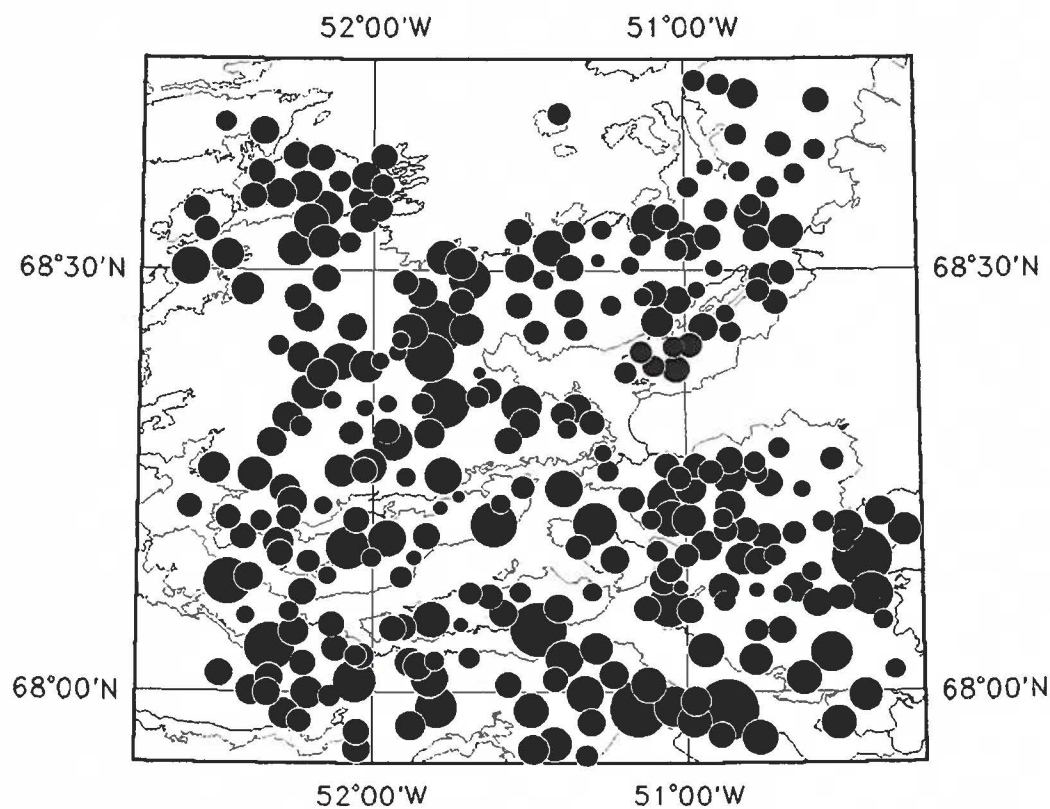
X-ray Fluorescence Analysis

Number of samples:	286
Min. value:	51.0
Max. value:	70.9
Mean:	64.5
Median:	65.0
Variance:	13.4
Std. Dev.:	3.7

50 km



Fig. 3



X-ray Fluorescence Analysis

Number of samples:	286
Min. value:	0.27
Max. value:	0.91
Mean:	0.46
Median:	0.45
Variance:	0.01
Std. Dev.:	0.09

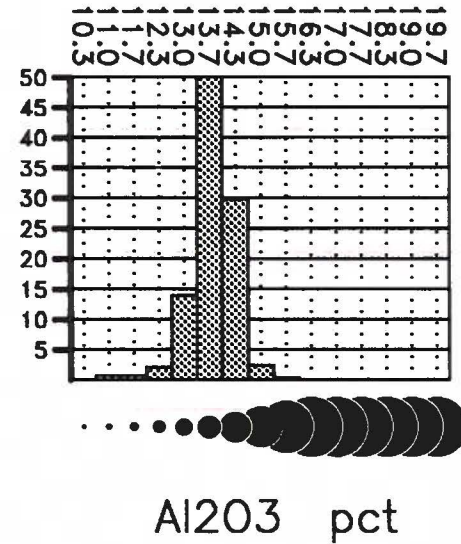
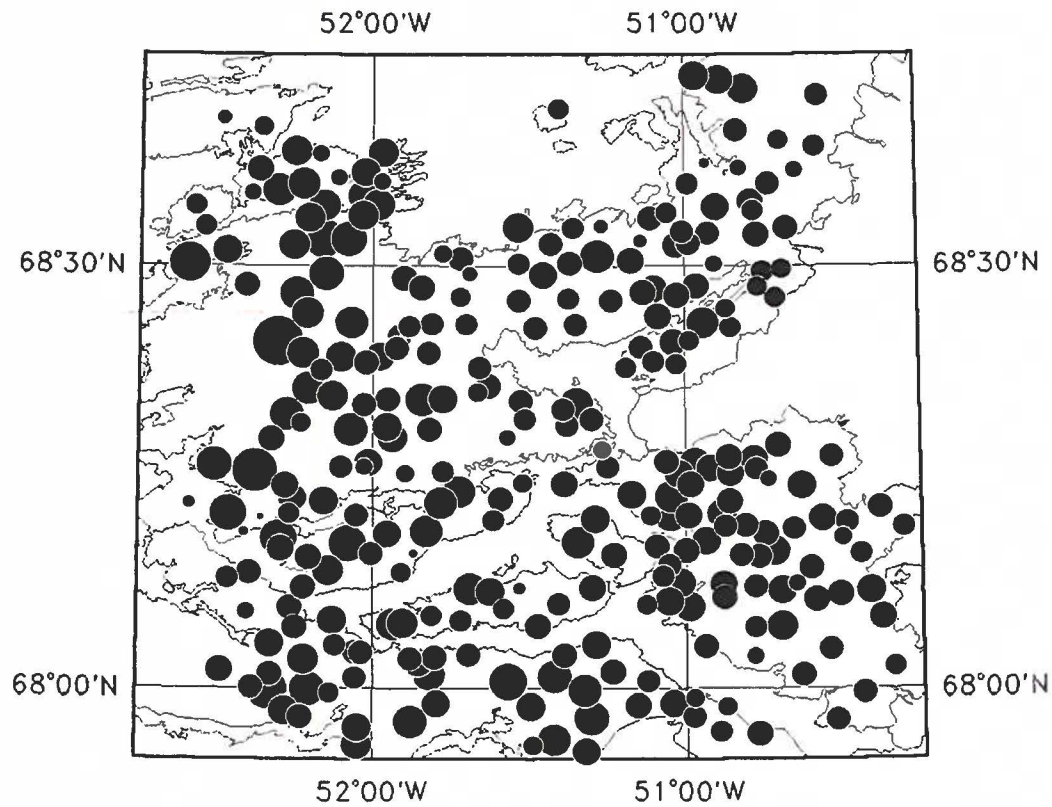
50 km



Fig. 4

Grønlands Geologiske Undersøgelse

GEOCHEMICAL MAP: Al₂O₃ in stream sediment



X-ray Fluorescence Analysis

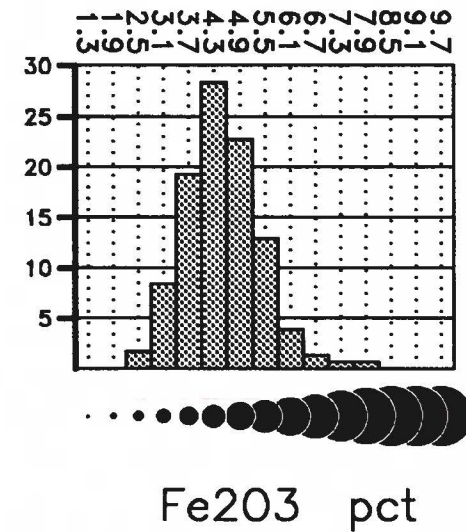
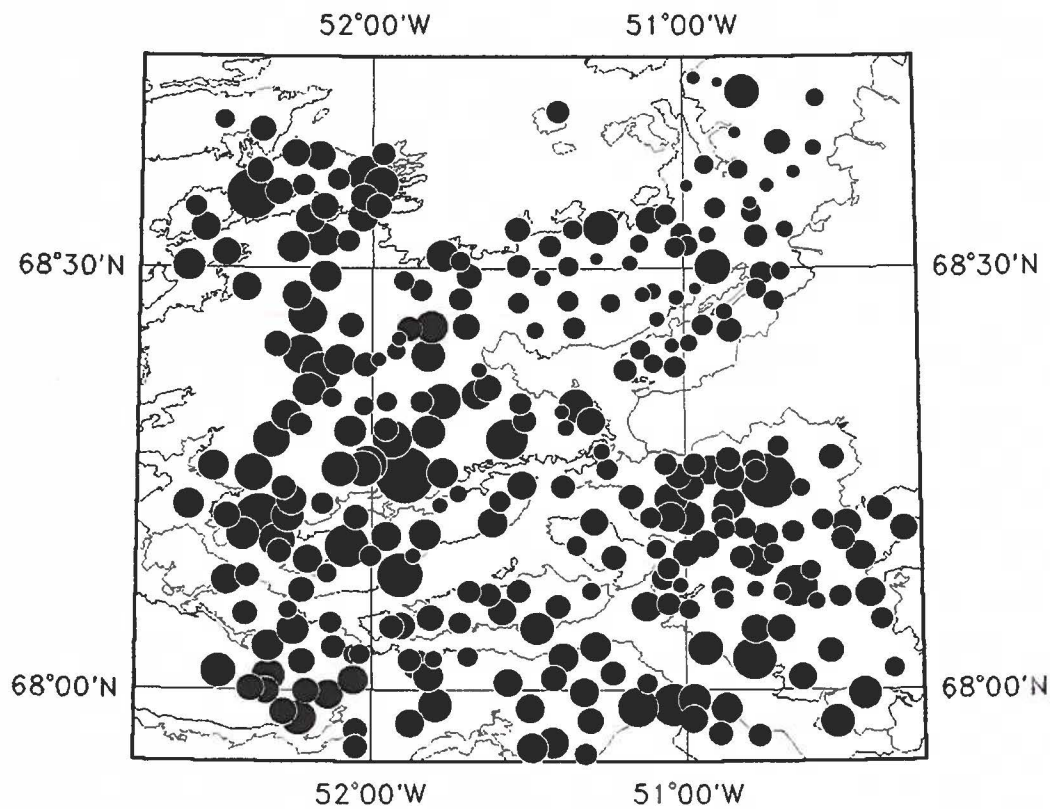
Number of samples: 286
Min. value: 10.8
Max. value: 15.5
Mean: 13.7
Median: 13.8
Variance: 0.3
Std. Dev.: 0.6

50 km

Fig. 5

Grønlands Geologiske Undersøgelse

GEOCHEMICAL MAP: Fe₂O₃ in stream sediment

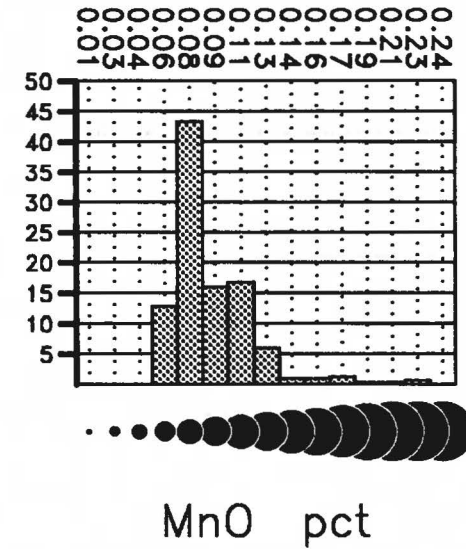
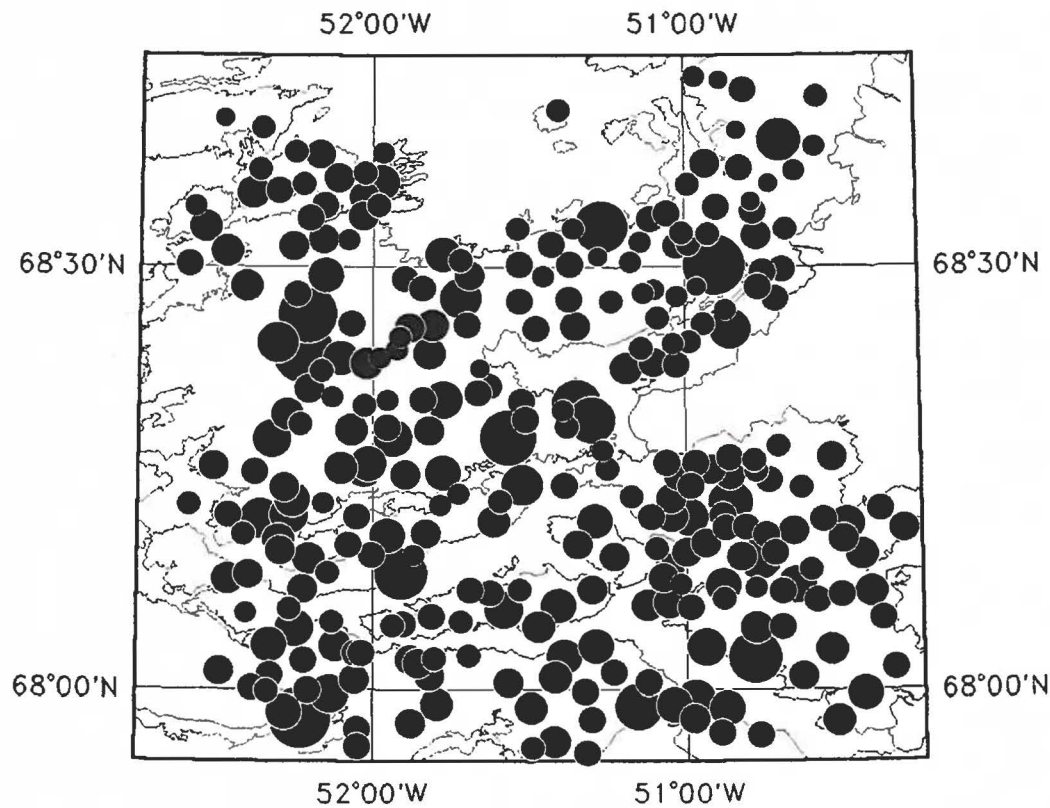


X-ray Fluorescence Analysis

Number of samples:	286
Min. value:	2.5
Max. value:	7.8
Mean:	4.5
Median:	4.4
Variance:	0.8
Std. Dev.:	0.9

50 km

Fig. 6



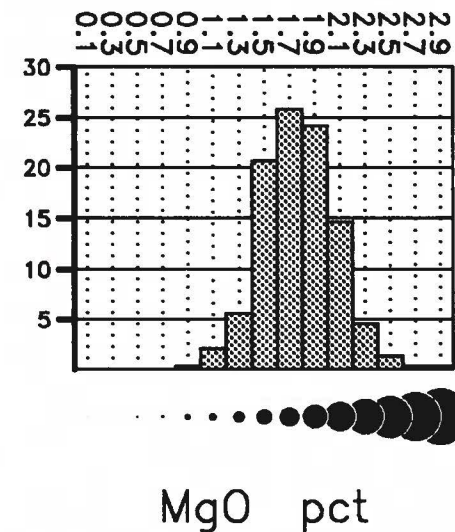
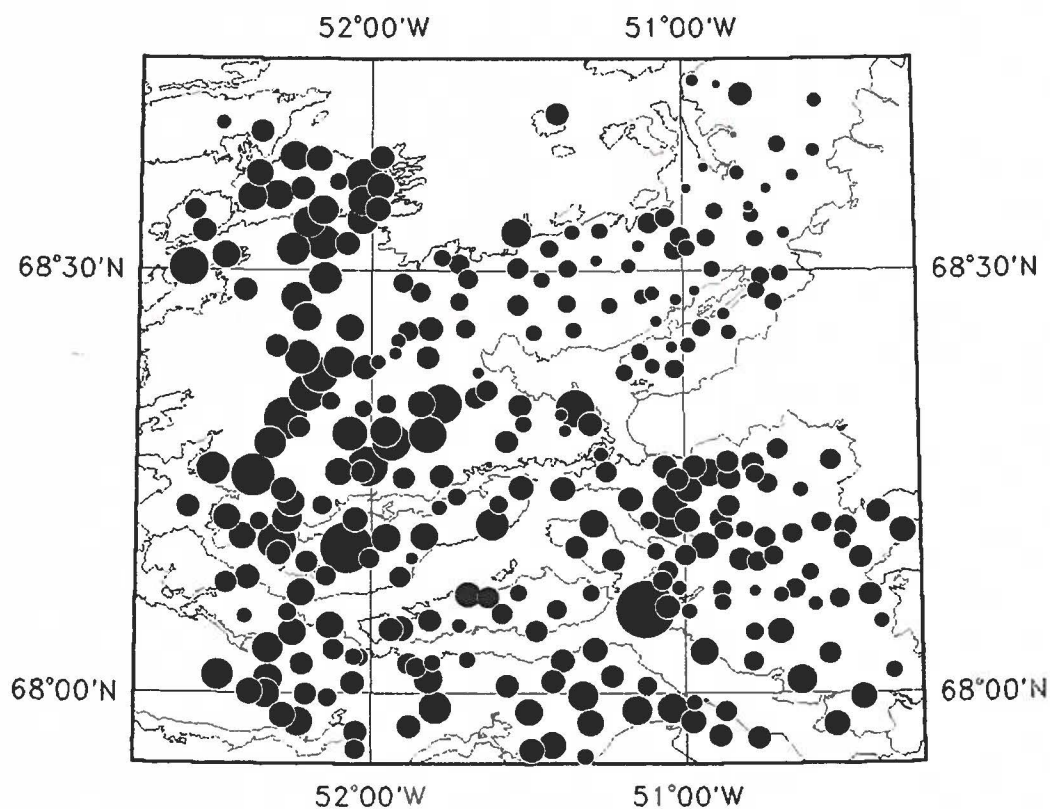
X-ray Fluorescence Analysis

Number of samples:	286
Min. value:	0.05
Max. value:	0.23
Mean:	0.09
Median:	0.08
Variance:	0.00
Std. Dev.:	0.03



Fig. 7

GEOCHEMICAL MAP: MgO in stream sediment



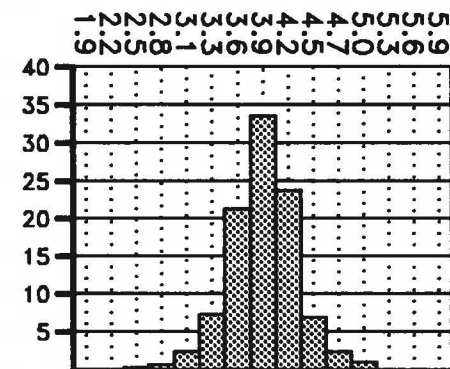
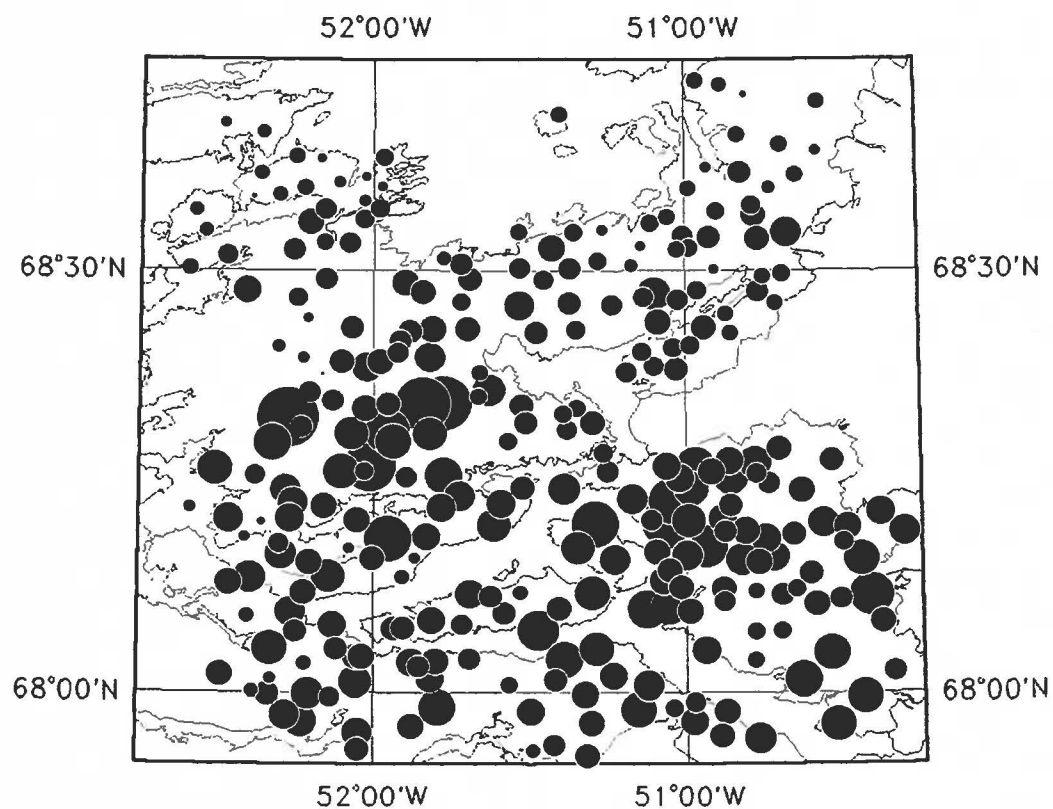
X-ray Fluorescence Analysis

Number of samples:	286
Min. value:	0.9
Max. value:	2.9
Mean:	1.8
Median:	1.8
Variance:	0.1
Std. Dev.:	0.3

50 km

Fig. 8

GEOCHEMICAL MAP: CaO in stream sediment



CaO pct

X-ray Fluorescence Analysis

Number of samples:	286
Min. value:	2.4
Max. value:	5.0
Mean:	3.9
Median:	3.9
Variance:	0.1
Std. Dev.:	0.4

50 km

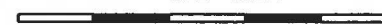
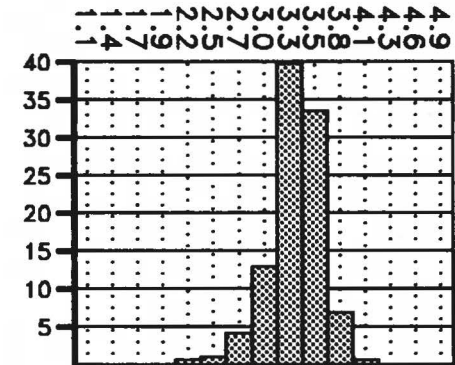
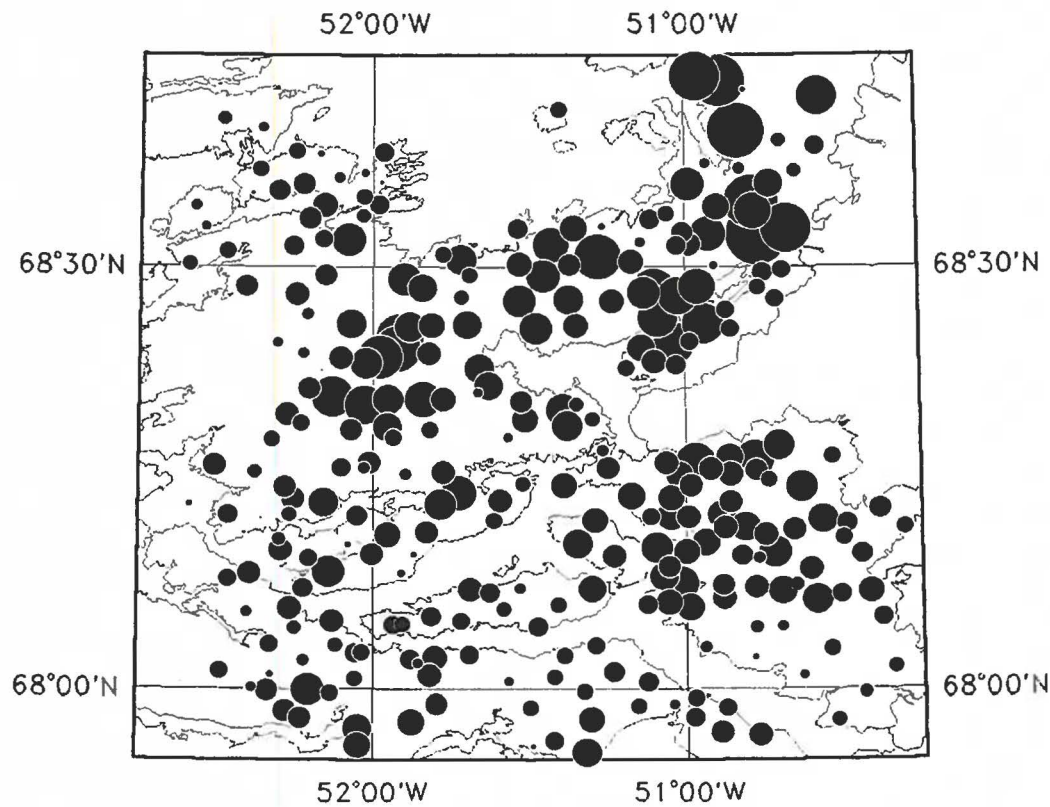


Fig. 9



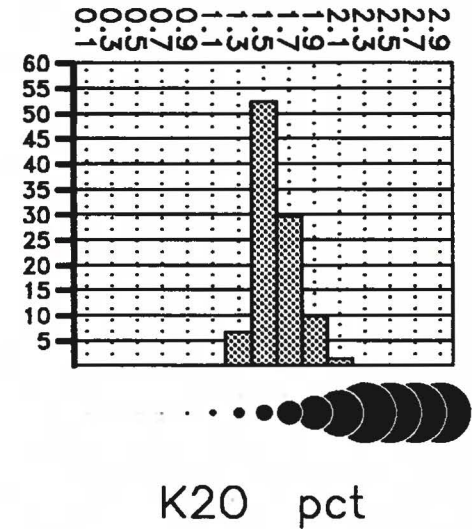
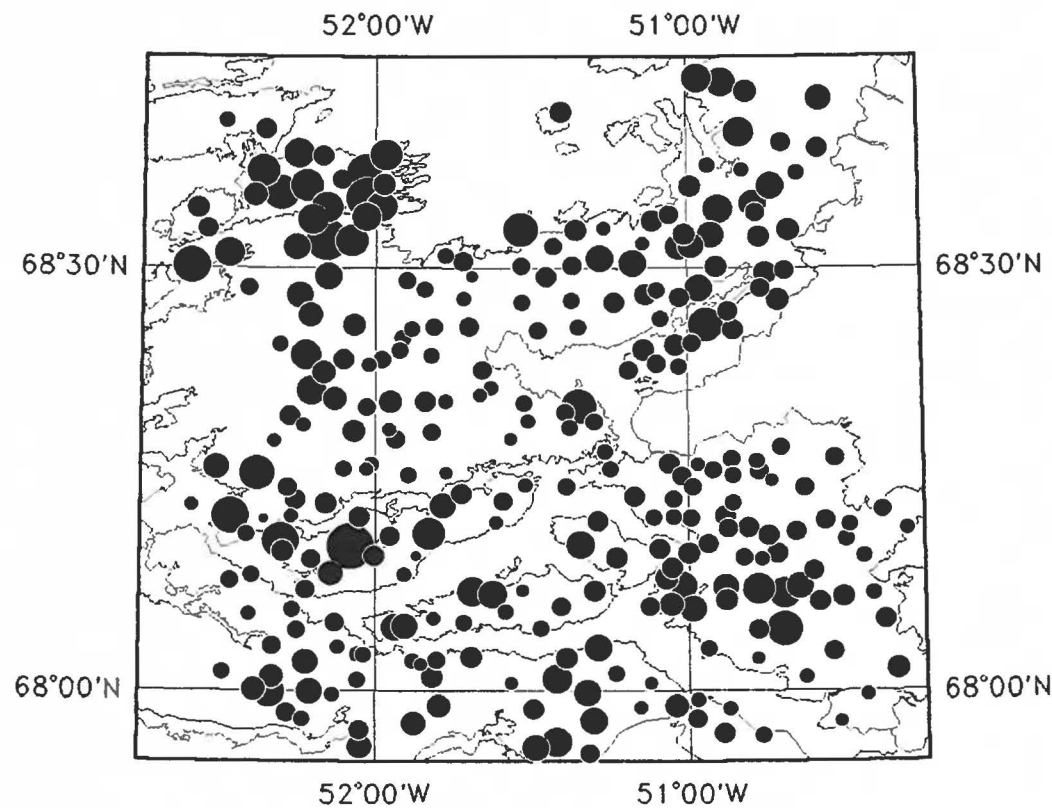
Na₂O pct

Atomic Absorption Spectrometry

Number of samples:	286
Min. value:	2.2
Max. value:	4.0
Mean:	3.3
Median:	3.3
Variance:	0.1
Std. Dev.:	0.3

50 km

Fig. 10



X-ray Fluorescence Analysis

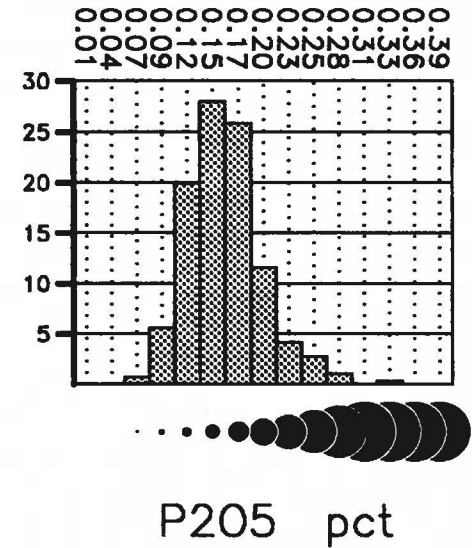
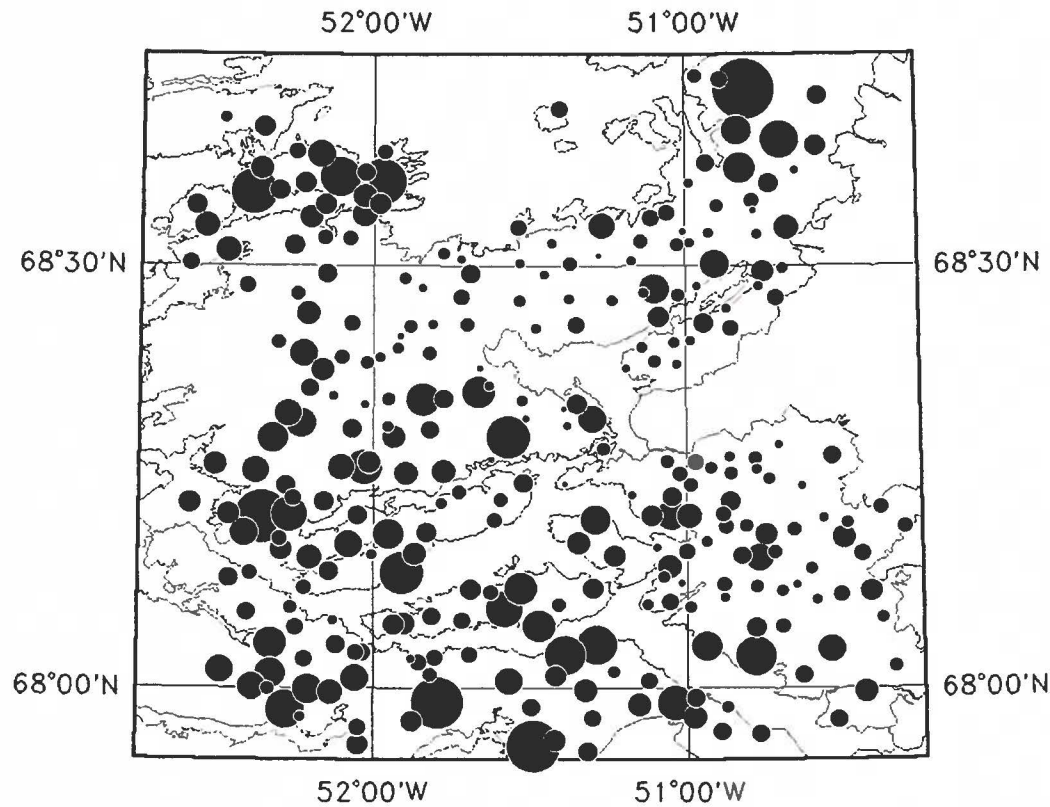
Number of samples:	286
Min. value:	1.2
Max. value:	2.1
Mean:	1.6
Median:	1.6
Variance:	0.0
Std. Dev.:	0.2

50 km

Fig. 11



GEOCHEMICAL MAP: P205 in stream sediment



X-ray Fluorescence Analysis

Number of samples:	286
Min. value:	0.06
Max. value:	0.33
Mean:	0.16
Median:	0.16
Variance:	0.00
Std. Dev.:	0.04

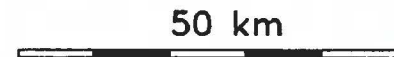
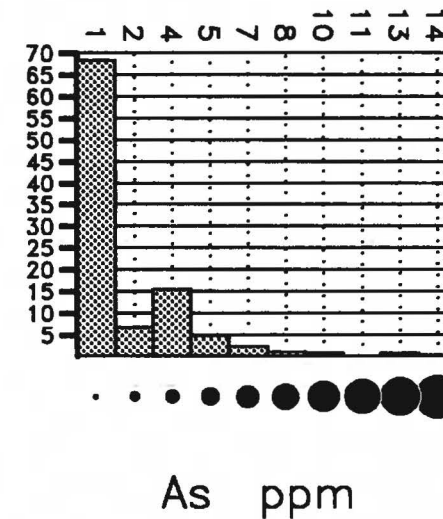
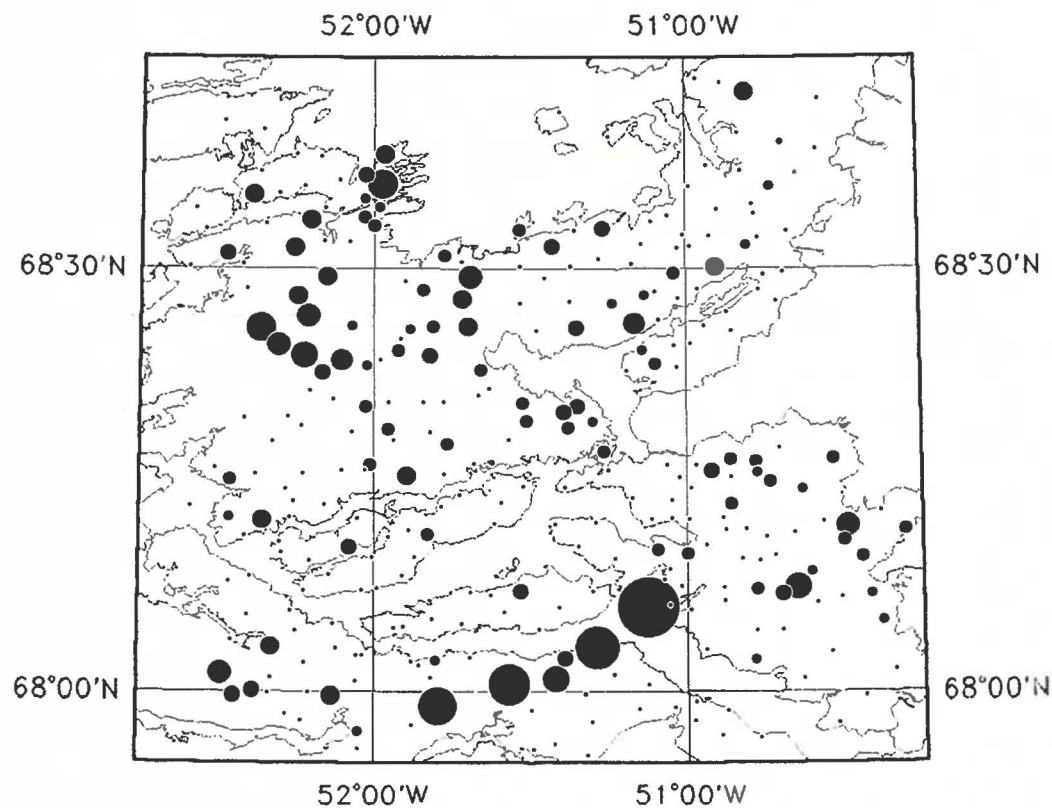


Fig. 12



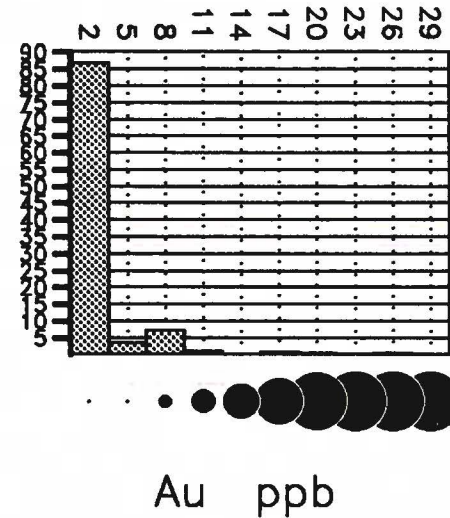
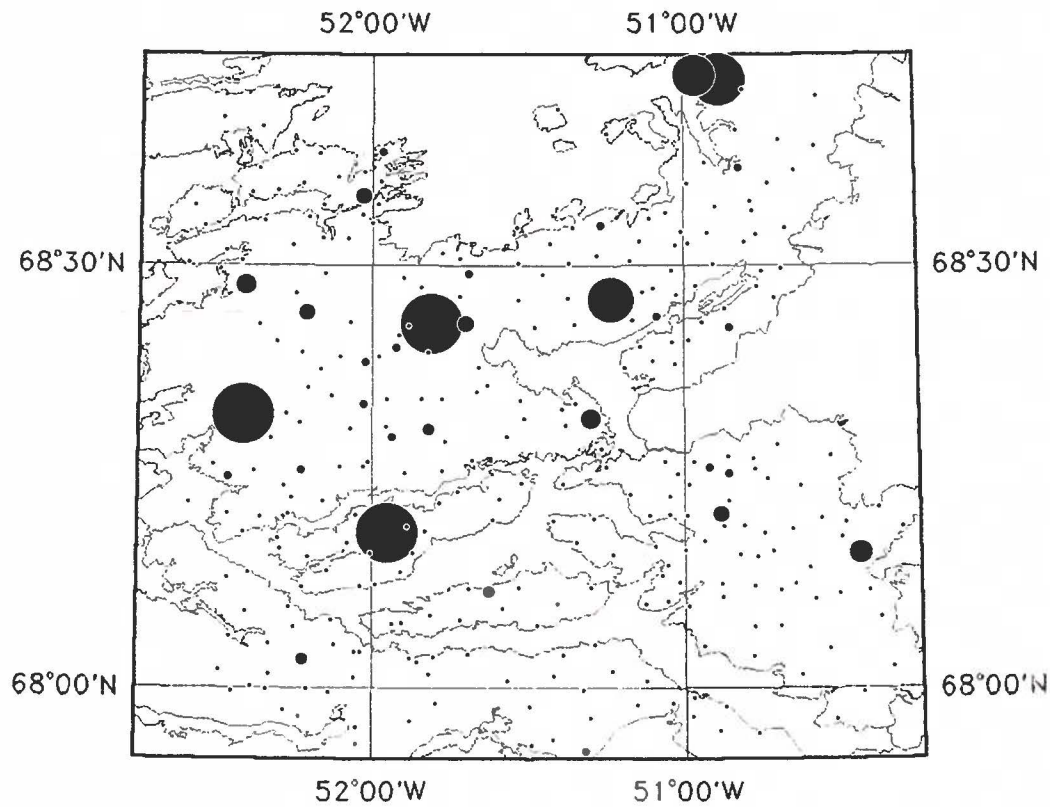
Instrumental Neutron Activation Analysis

Number of samples:	305
Min. value:	0
Max. value:	62
Mean:	2
Median:	0
Variance:	17
Std. Dev.:	4

50 km



Fig. 13



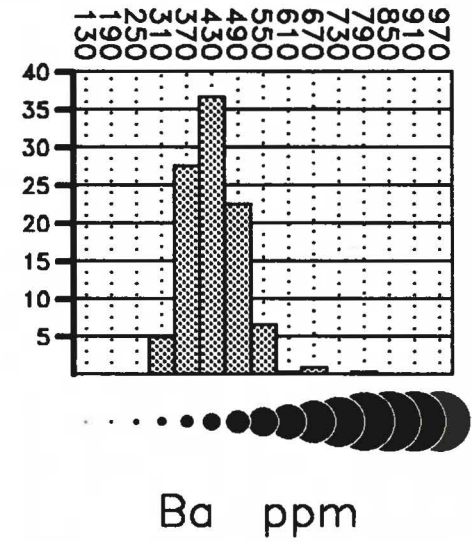
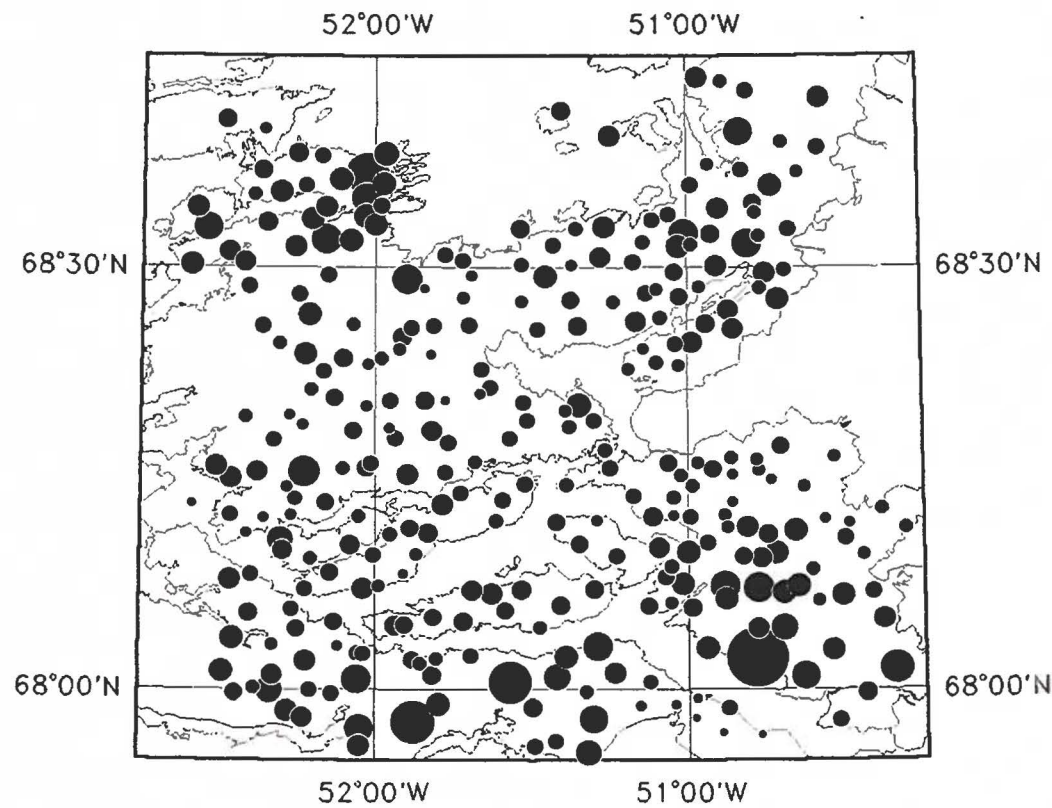
Instrumental Neutron Activation Analysis

Number of samples:	305
Min. value:	0
Max. value:	115
Mean:	2
Median:	0
Variance:	76
Std. Dev.:	9

50 km



Fig. 14



Instrumental Neutron Activation Analysis

Number of samples:	305
Min. value:	280
Max. value:	810
Mean:	427
Median:	420
Variance:	4419
Std. Dev.:	66

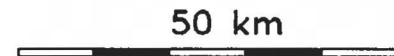
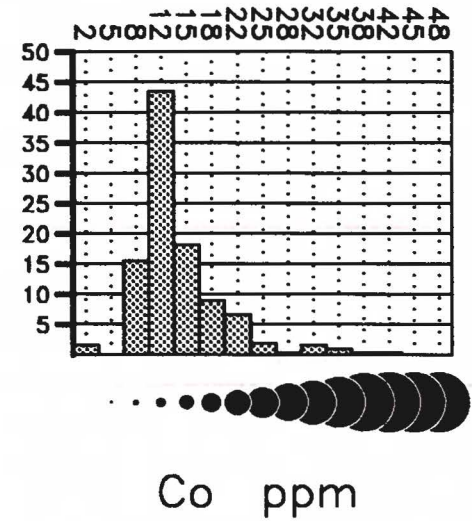
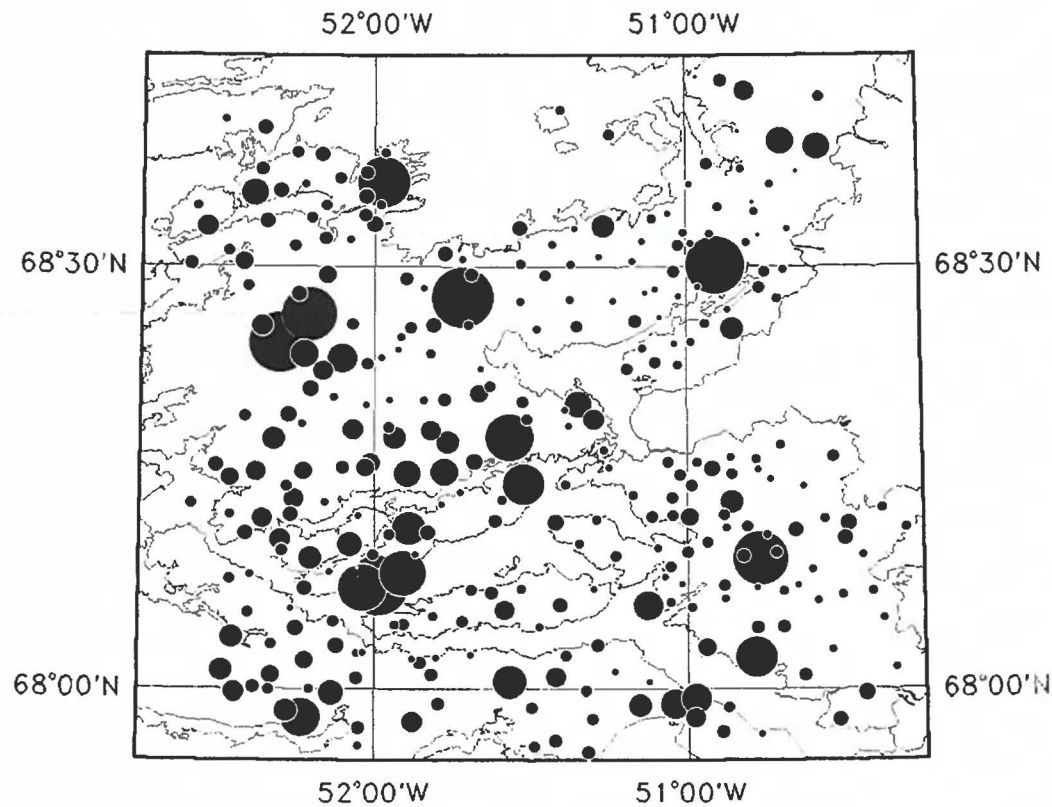


Fig. 15

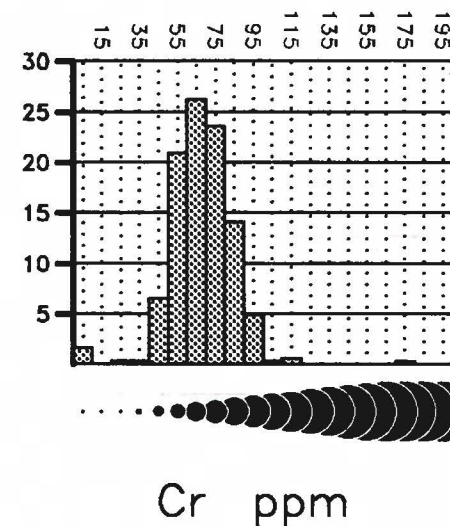
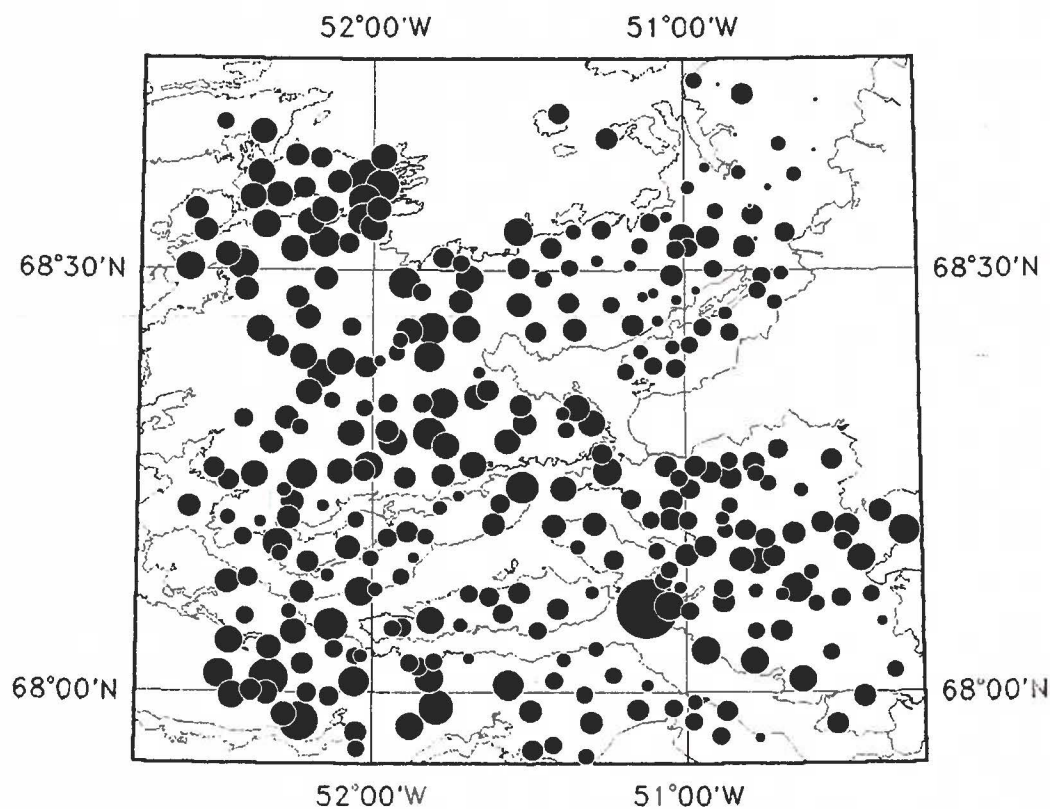


Instrumental Neutron Activation Analysis

Number of samples:	305
Min. value:	0
Max. value:	61
Mean:	14
Median:	12
Variance:	47
Std. Dev.:	7



Fig. 16



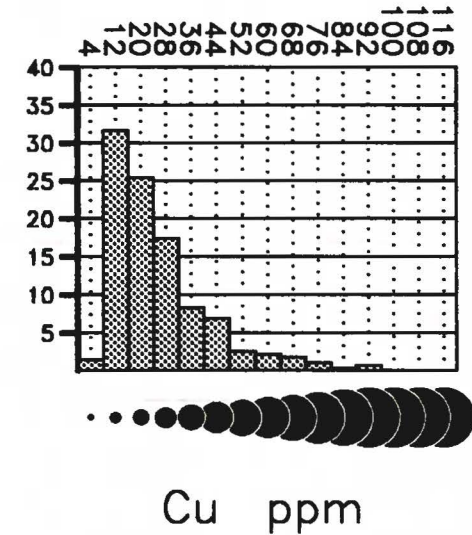
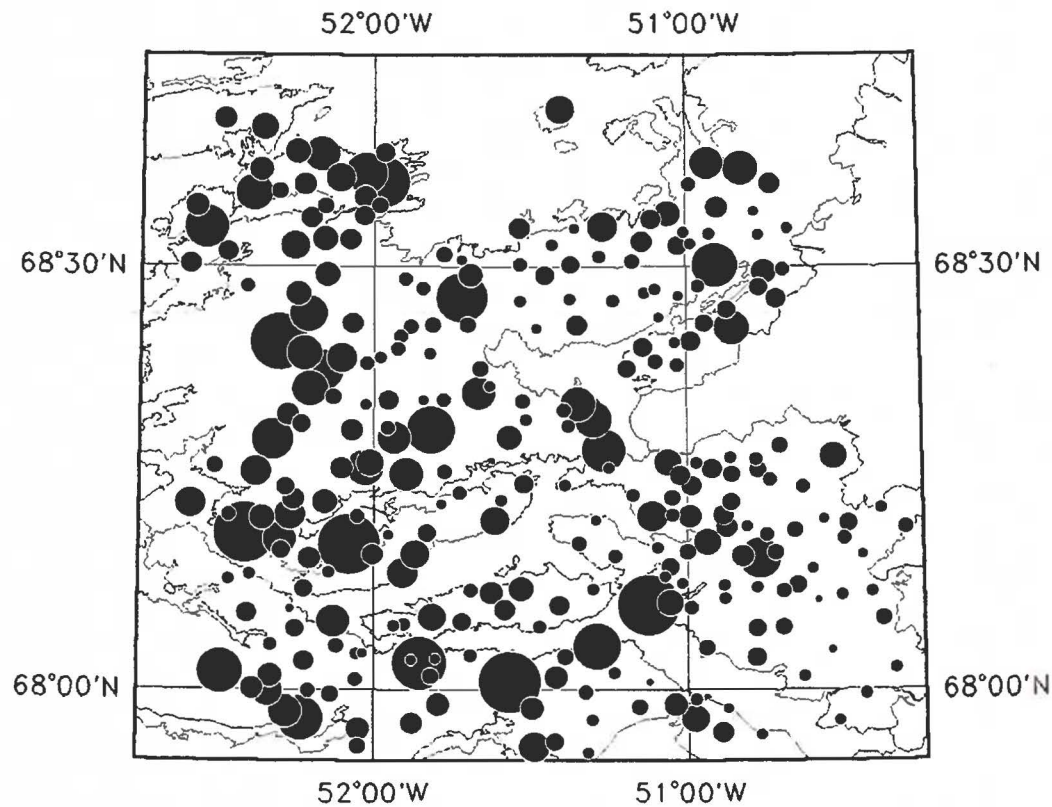
Instrumental Neutron Activation Analysis

Number of samples:	305
Min. value:	0
Max. value:	170
Mean:	67
Median:	67
Variance:	284
Std. Dev.:	17

50 km



Fig. 17



Atomic Absorption Analysis

Number of samples:	277
Min. value:	4
Max. value:	161
Mean:	26
Median:	21
Variance:	380
Std. Dev.:	19

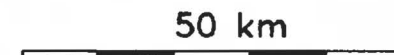
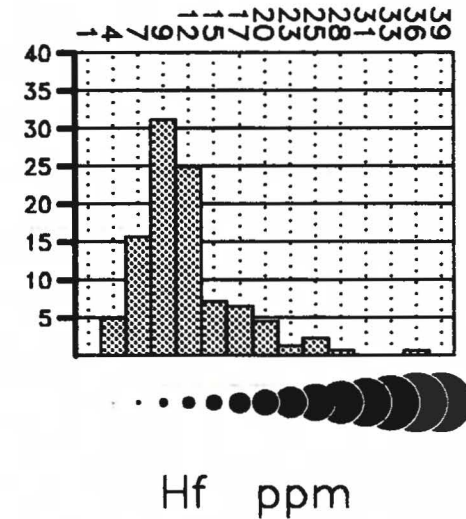
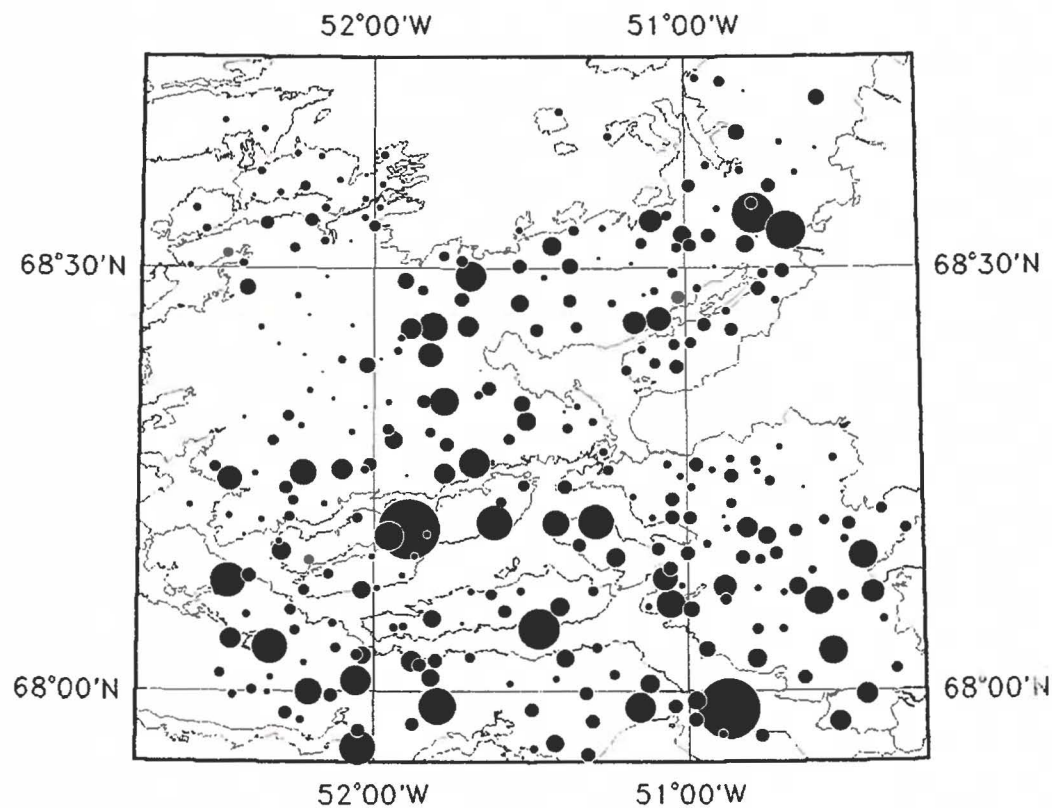


Fig. 18

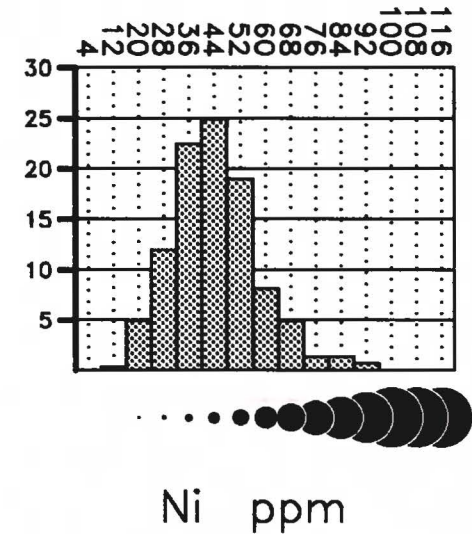
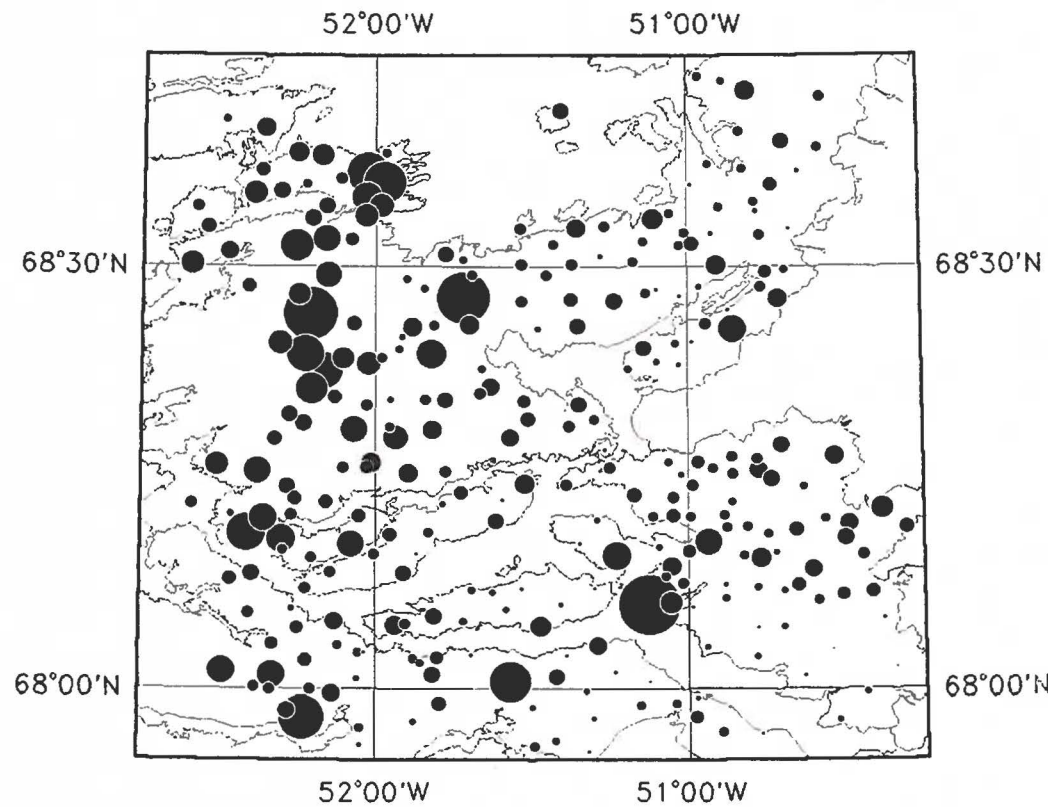


Instrumental Neutron Activation Analysis

Number of samples:	305
Min. value:	3
Max. value:	36
Mean:	11
Median:	10
Variance:	25
Std. Dev.:	5



Fig. 19

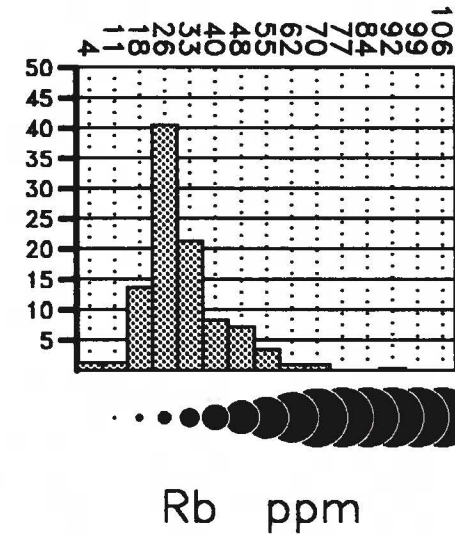
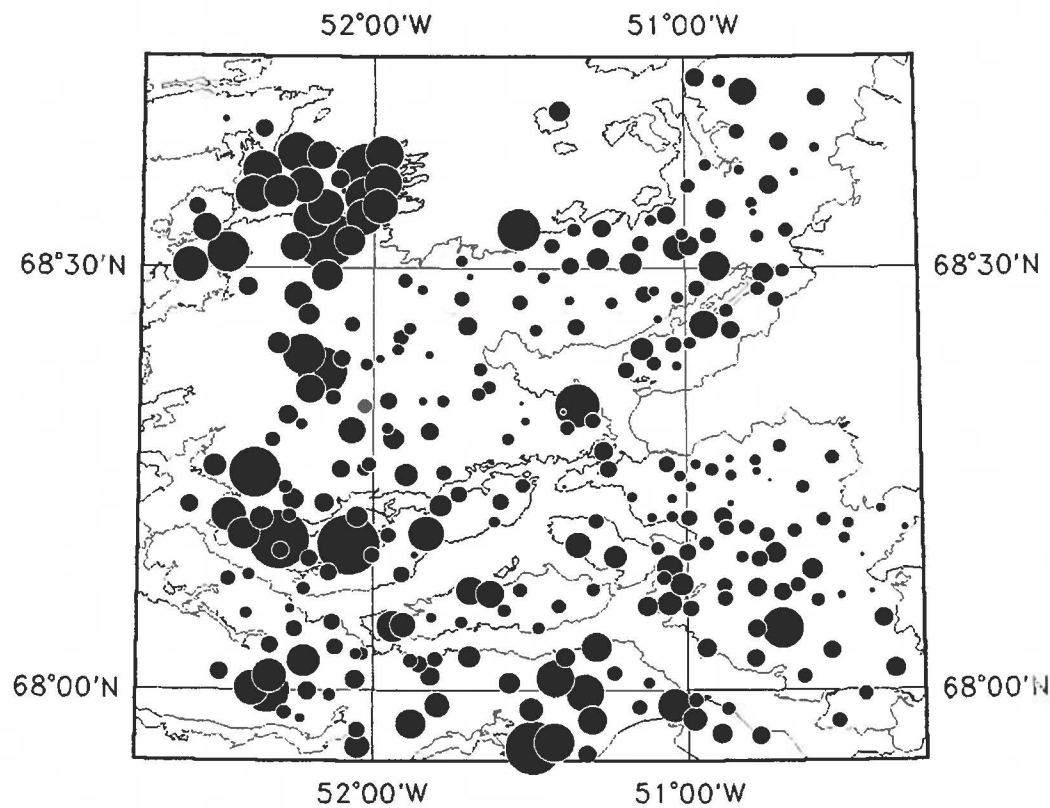


X-ray Fluorescence Analysis

Number of samples:	286
Min. value:	16
Max. value:	216
Mean:	45
Median:	43
Variance:	289
Std. Dev.:	17



Fig. 20



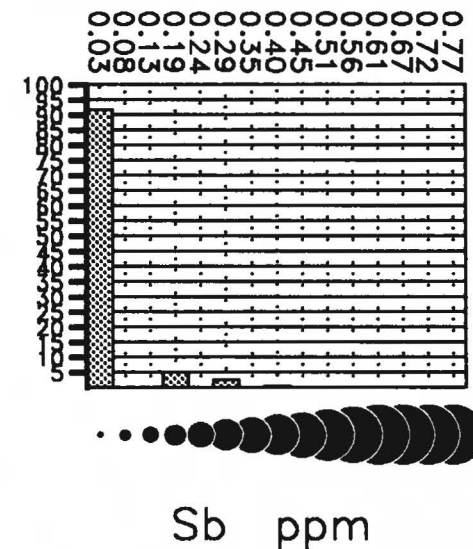
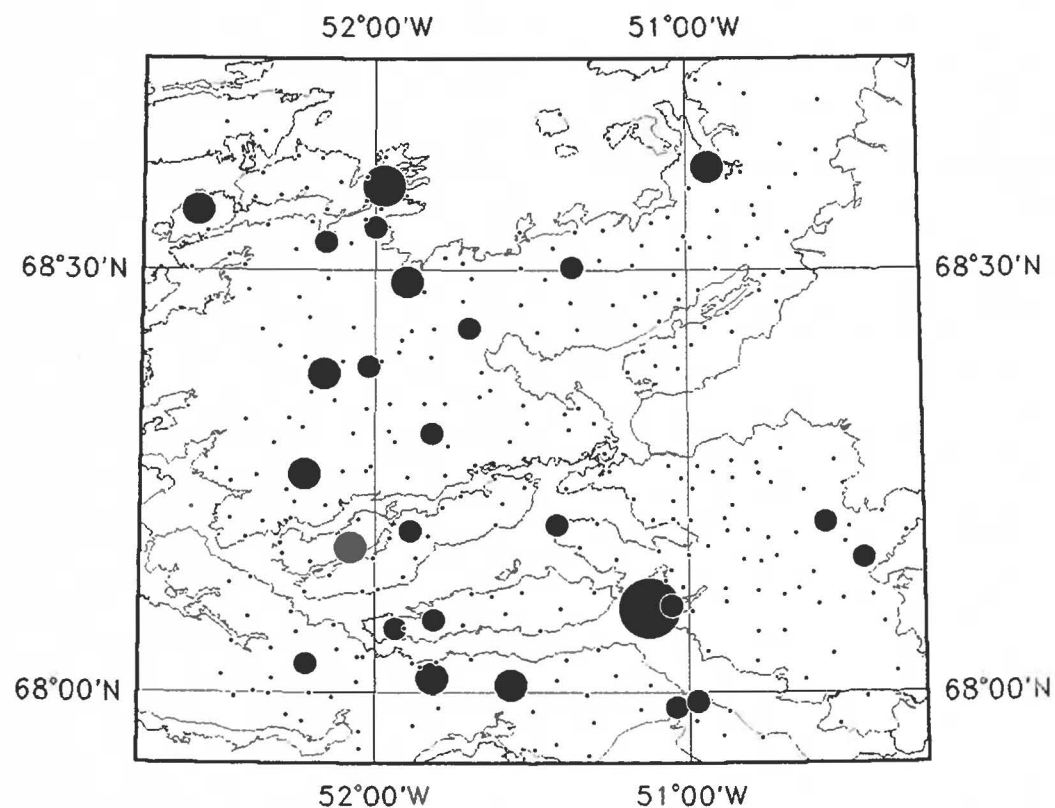
X-ray Fluorescence Analysis

Number of samples:	286
Min. value:	0
Max. value:	92
Mean:	31
Median:	28
Variance:	137
Std. Dev.:	12

50 km

Fig. 21

GEOCHEMICAL MAP: Sb in stream sediment

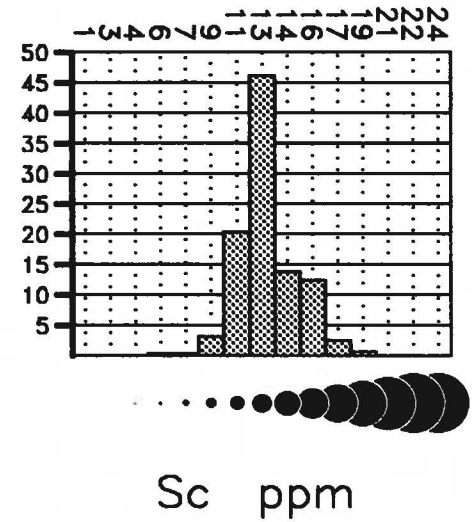
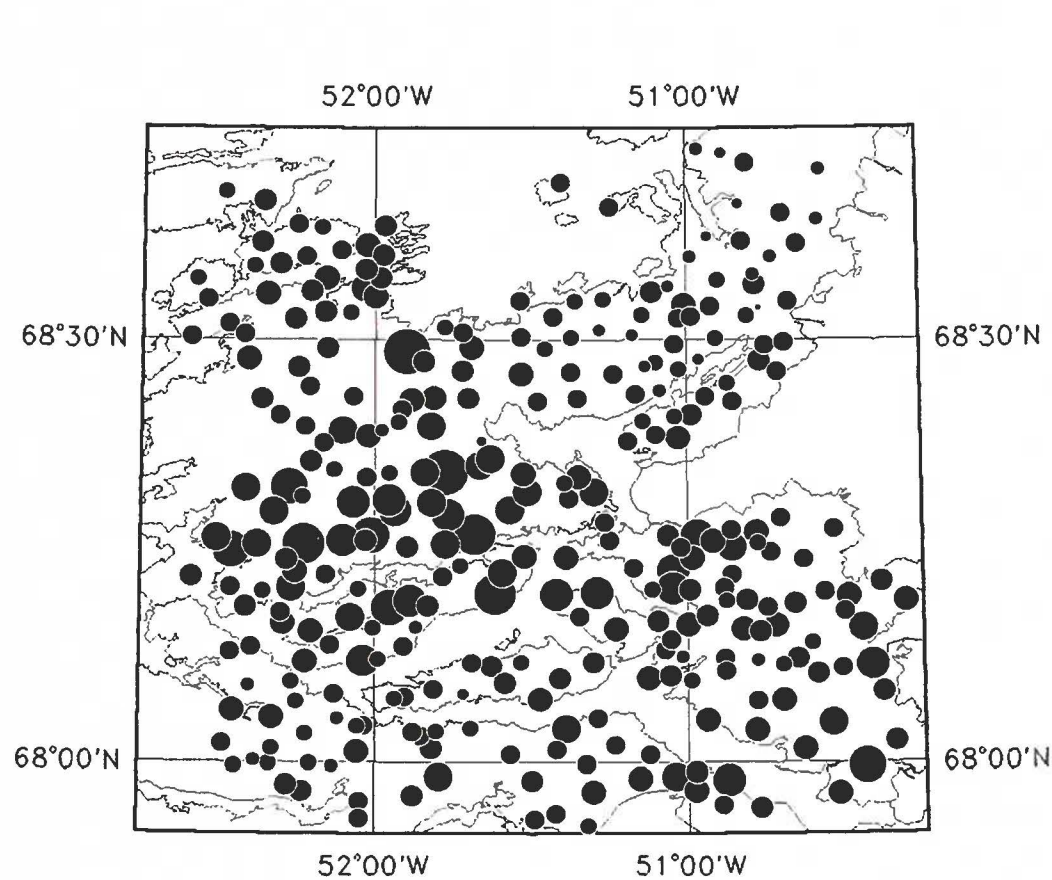


Instrumental Neutron Activation Analysis

Number of samples:	305
Min. value:	0.00
Max. value:	1.20
Mean:	0.02
Median:	0.00
Variance:	0.01
Std. Dev.:	0.10



Fig. 22

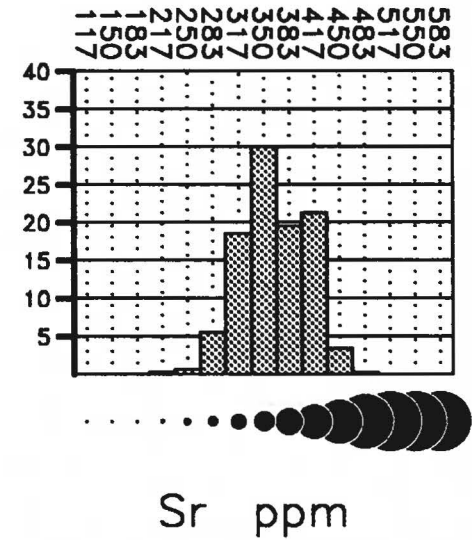
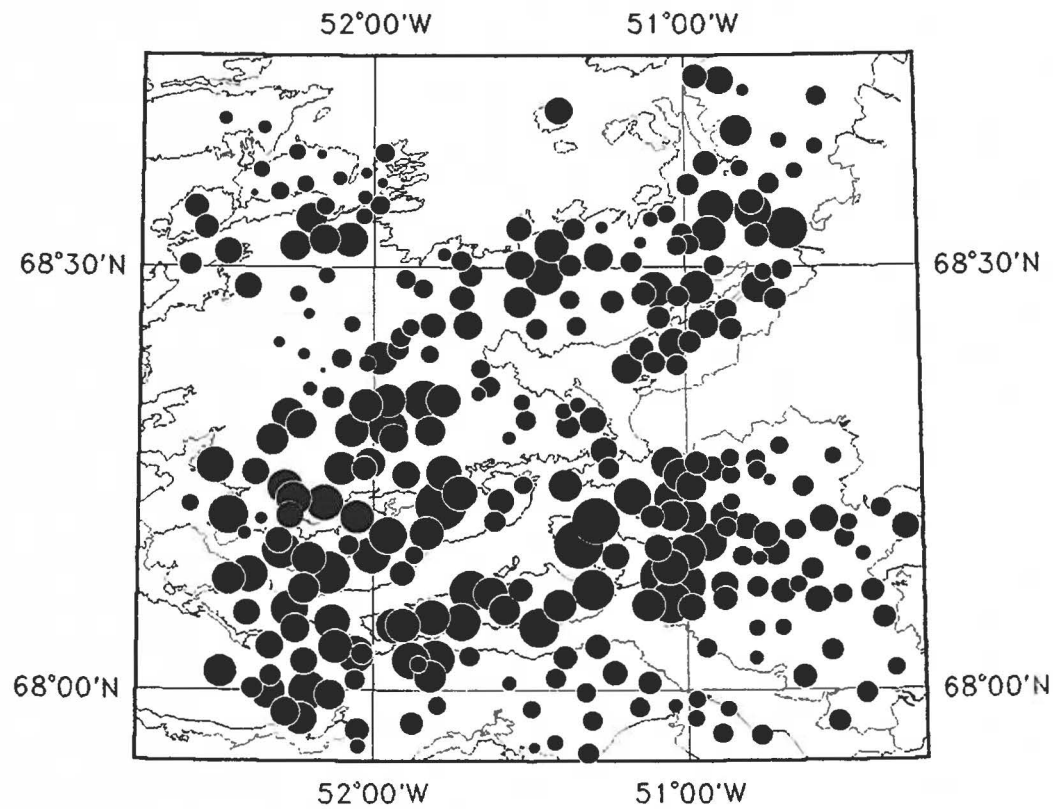


Instrumental Neutron Activation Analysis

Number of samples:	305
Min. value:	7
Max. value:	19
Mean:	13
Median:	12
Variance:	4
Std. Dev.:	2



Fig. 23



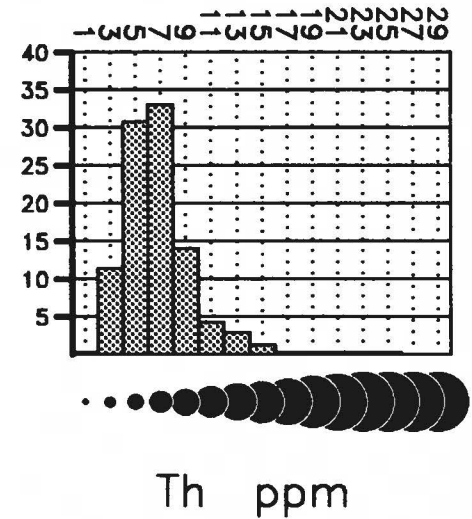
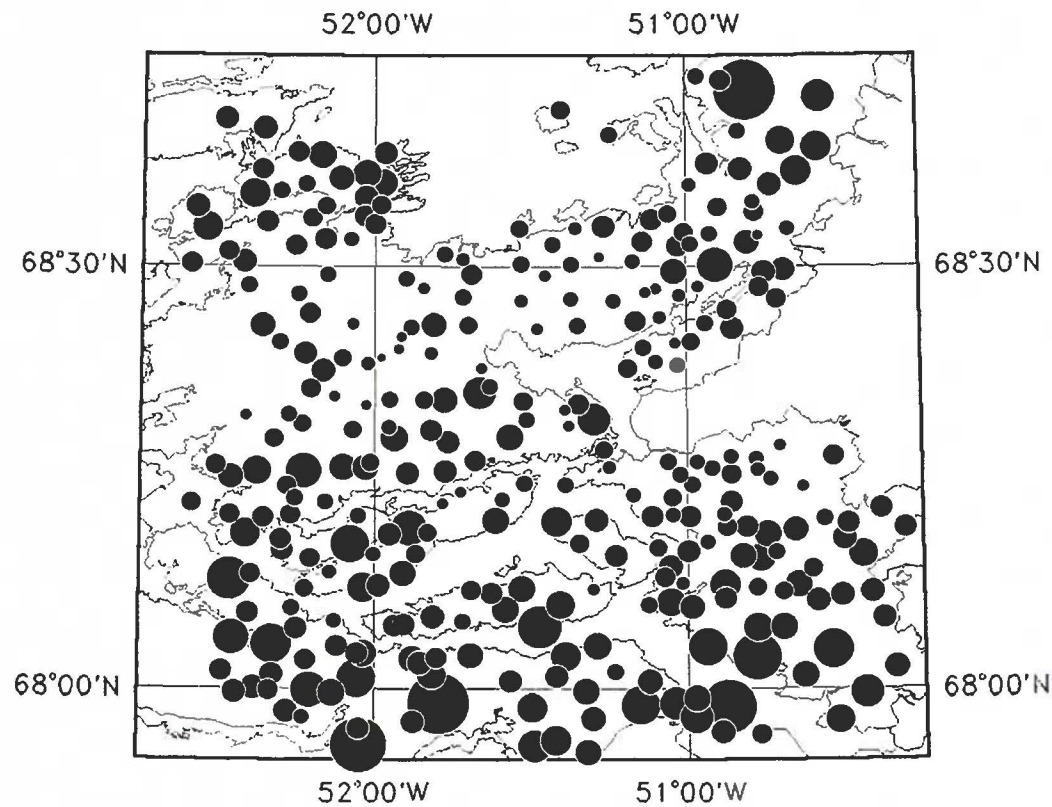
X-ray Fluorescence Analysis

Number of samples:	286
Min. value:	211
Max. value:	470
Mean:	363
Median:	358
Variance:	1899
Std. Dev.:	44

50 km



Fig. 24

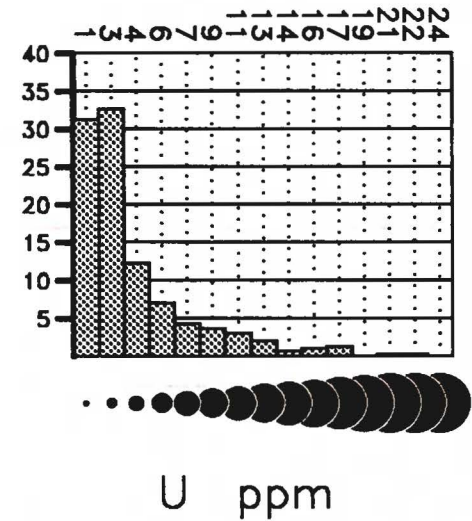
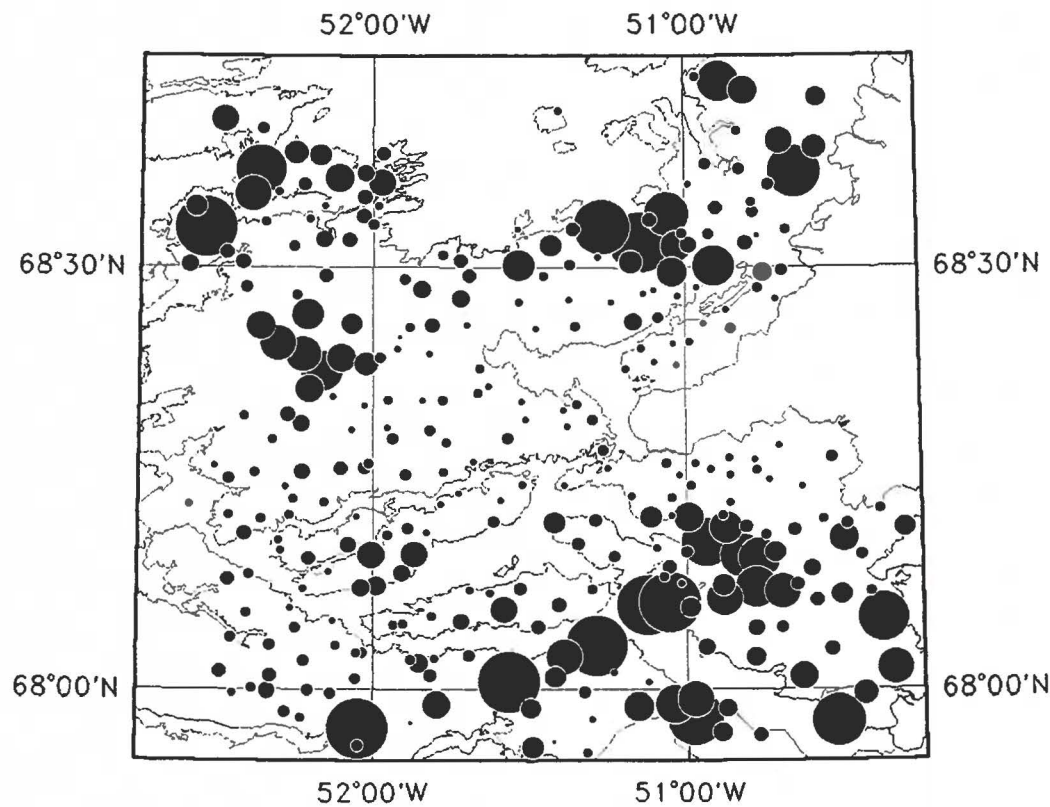


Instrumental Neutron Activation Analysis

Number of samples:	305
Min. value:	1
Max. value:	24
Mean:	7
Median:	6
Variance:	9
Std. Dev.:	3

50 km

Fig. 25

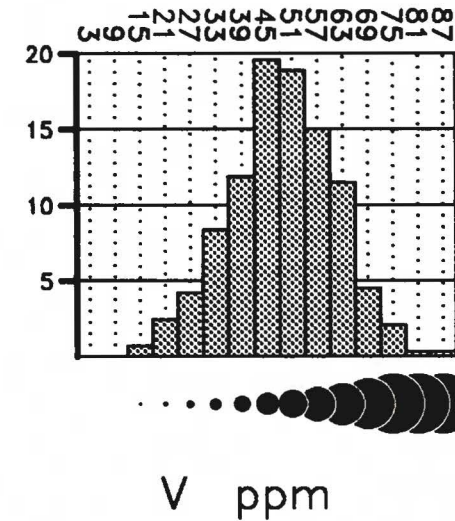
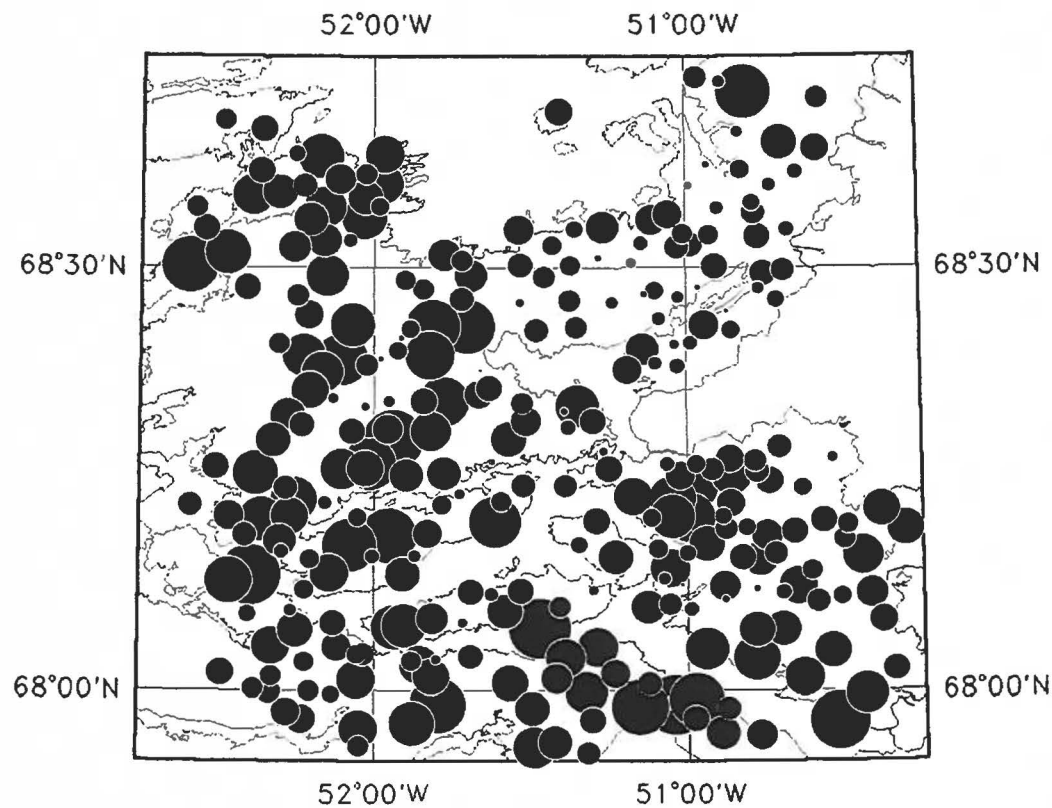


Instrumental Neutron Activation Analysis

Number of samples:	305
Min. value:	0
Max. value:	60
Mean:	5
Median:	3
Variance:	47
Std. Dev.:	7



Fig. 26



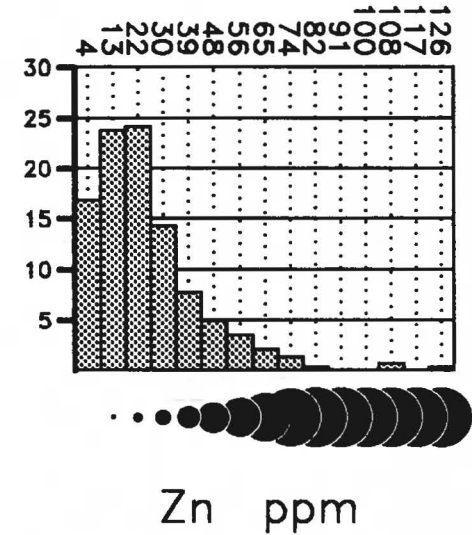
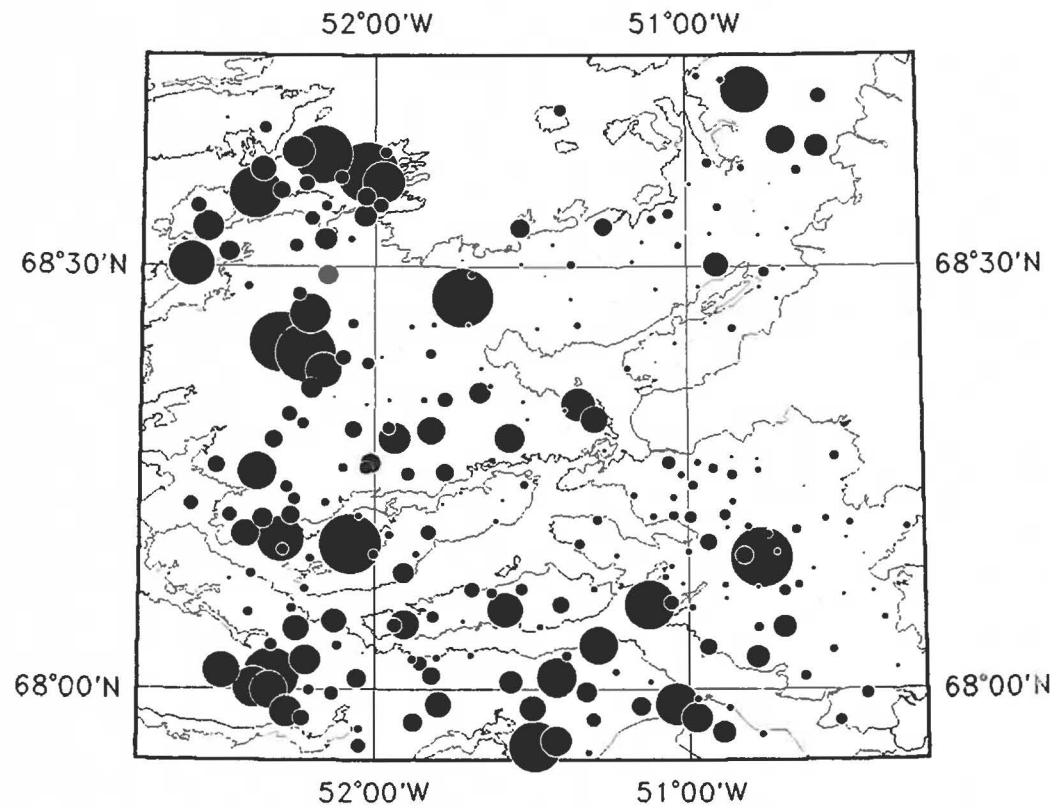
X-ray Fluorescence Analysis

Number of samples:	286
Min. value:	13
Max. value:	86
Mean:	49
Median:	48
Variance:	156
Std. Dev.:	12

50 km

Fig. 27

GEOCHEMICAL MAP: Zn in stream sediment



X-ray Fluorescence Analysis

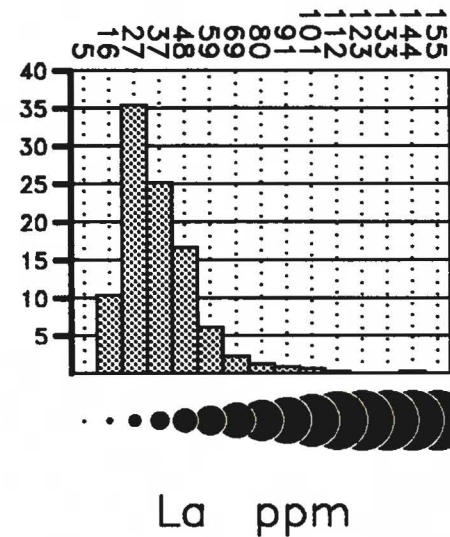
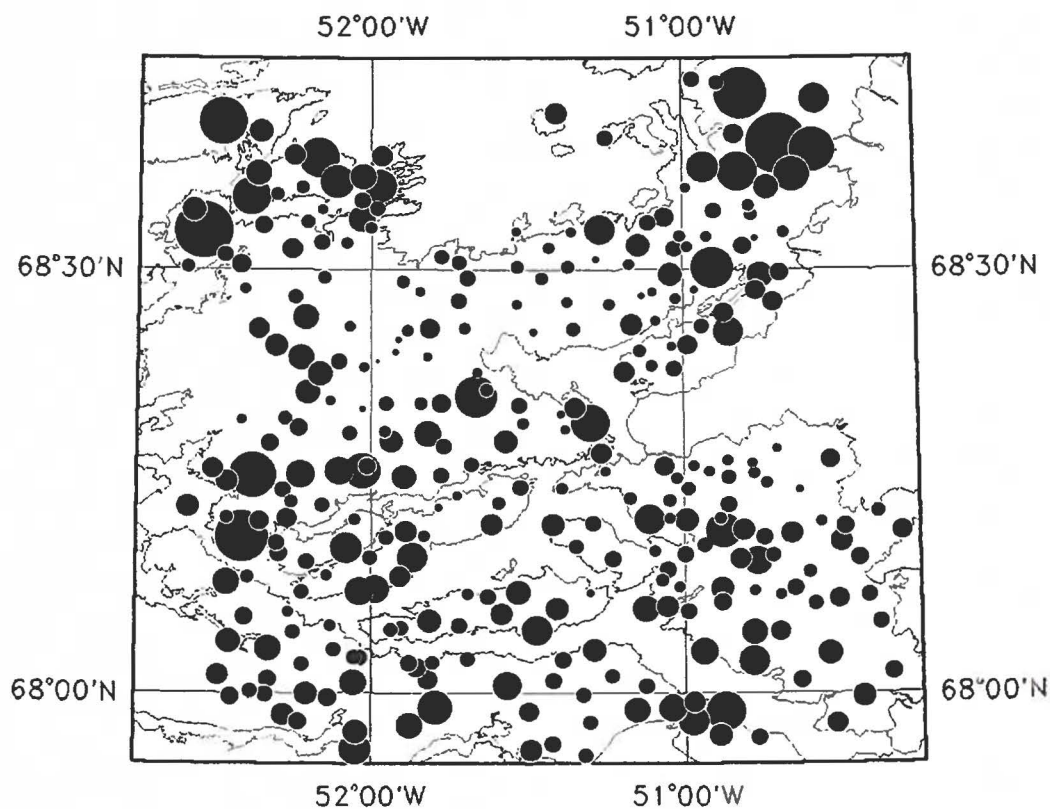
Number of samples:	286
Min. value:	0
Max. value:	123
Mean:	24
Median:	20
Variance:	351
Std. Dev.:	19

50 km



Fig. 28

GEOCHEMICAL MAP: La in stream sediment

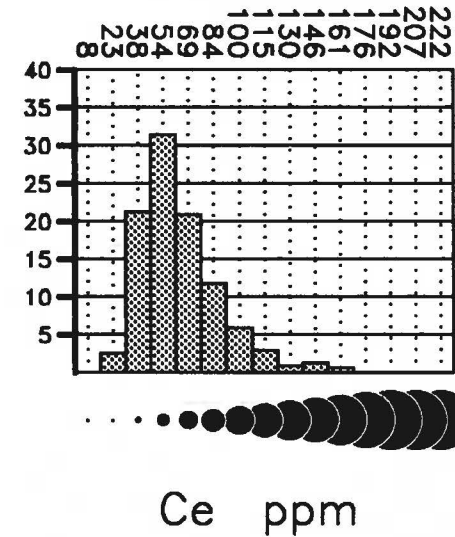
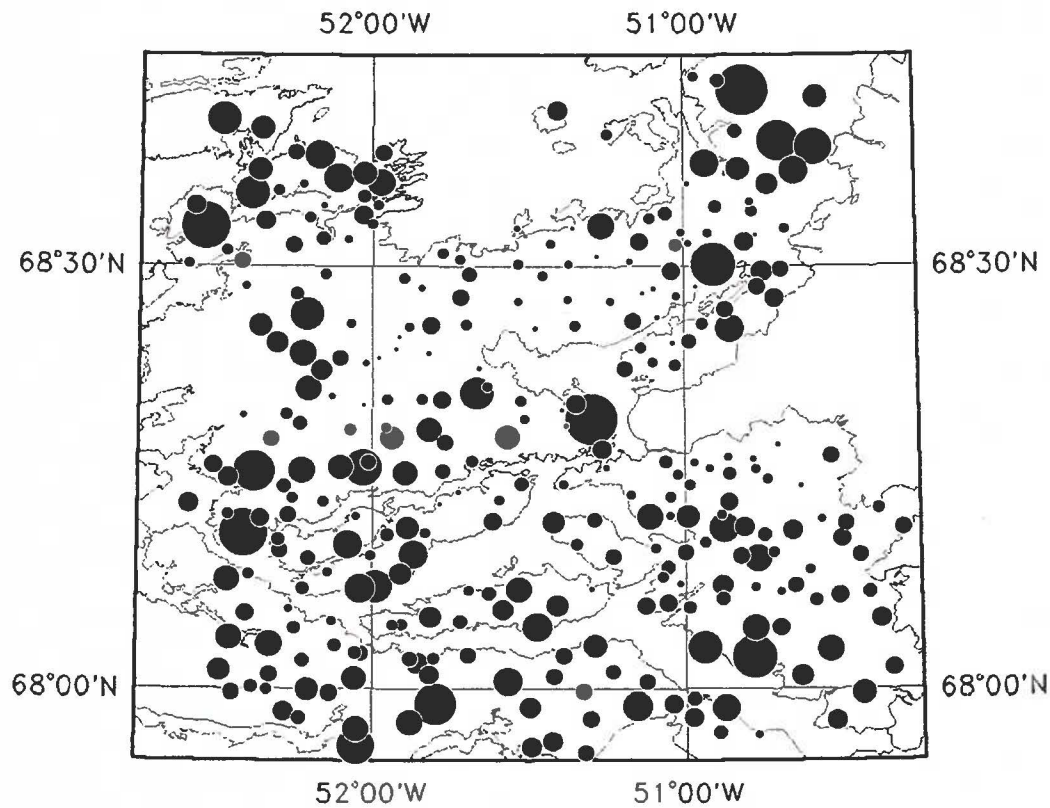


Instrumental Neutron Activation Analysis

Number of samples:	305
Min. value:	11
Max. value:	140
Mean:	37
Median:	32
Variance:	275
Std. Dev.:	17



Fig. 29



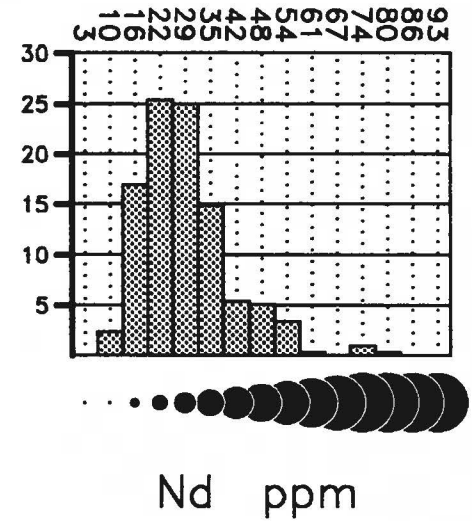
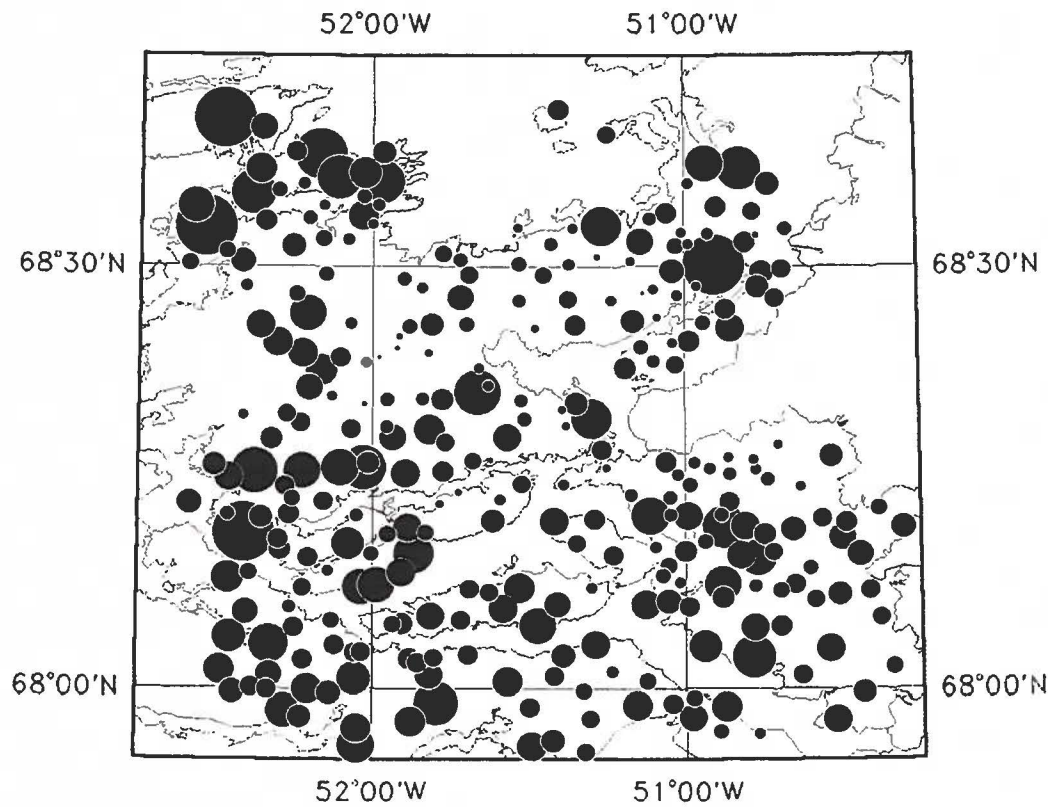
Instrumental Neutron Activation Analysis

Number of samples:	305
Min. value:	22
Max. value:	160
Mean:	63
Median:	59
Variance:	599
Std. Dev.:	24

50 km



Fig. 30

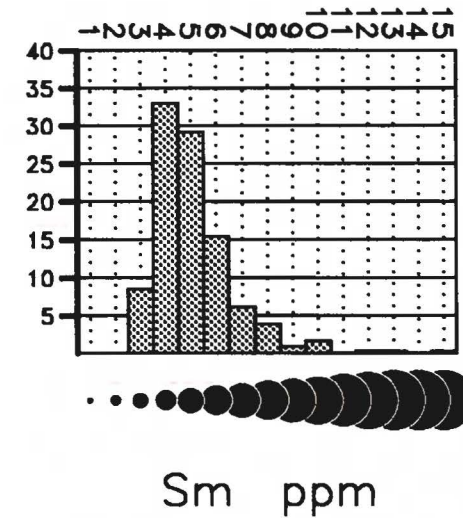
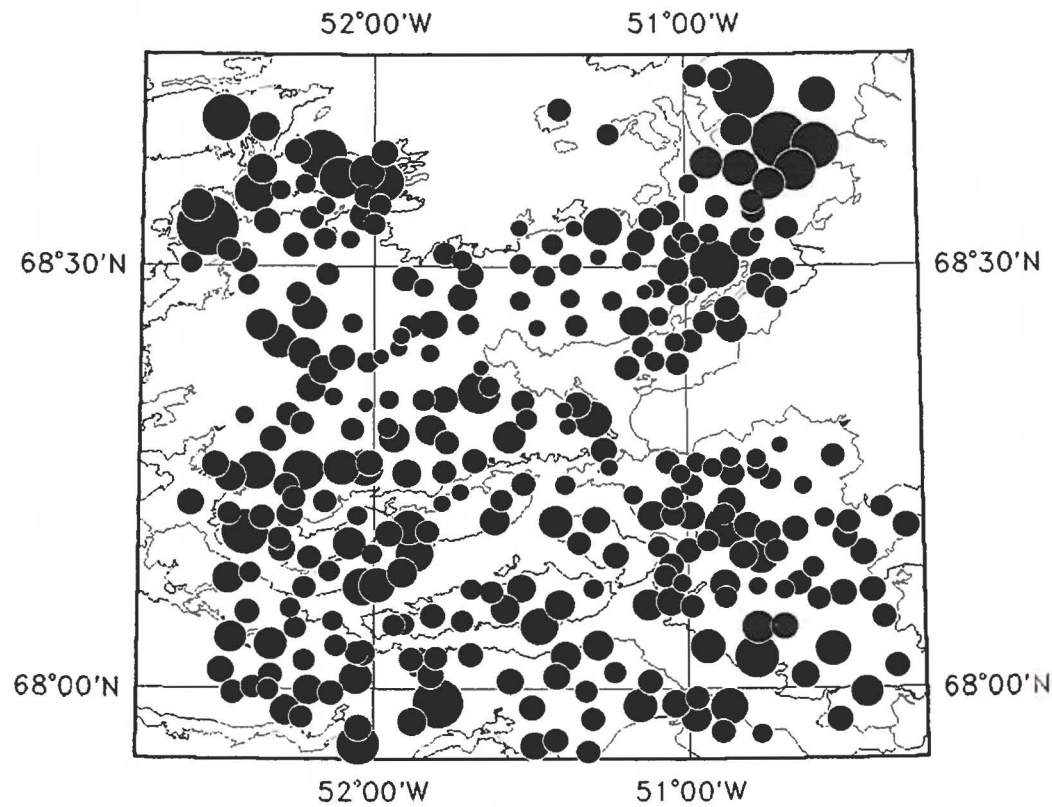


Instrumental Neutron Activation Analysis

Number of samples:	296
Min. value:	7
Max. value:	83
Mean:	29
Median:	27
Variance:	128
Std. Dev.:	11

50 km

Fig. 31

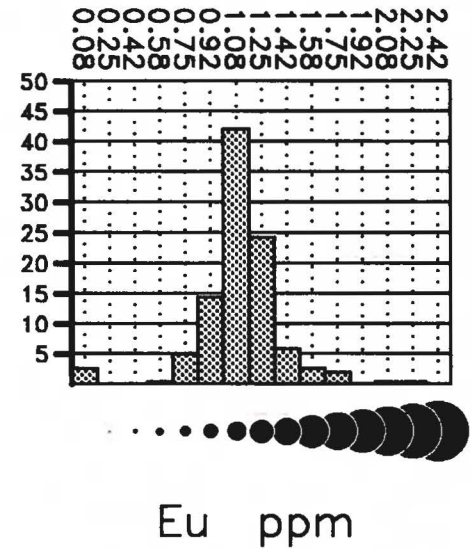
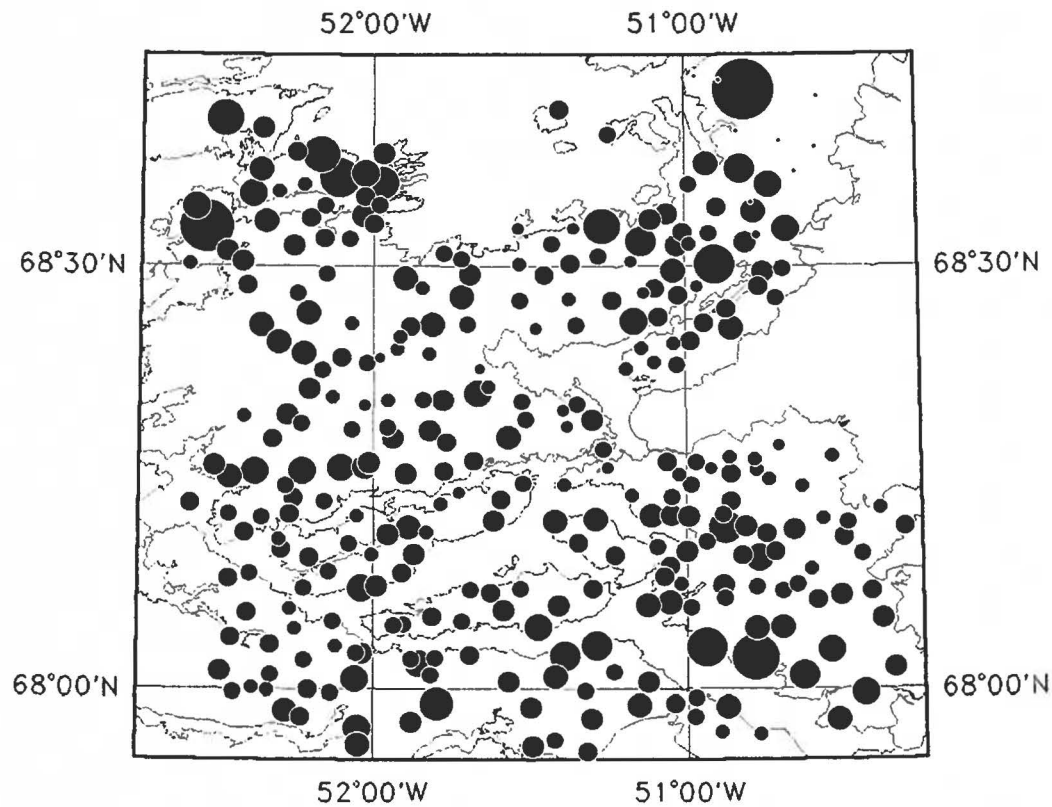


Instrumental Neutron Activation Analysis

Number of samples:	305
Min. value:	2
Max. value:	14
Mean:	5
Median:	4
Variance:	3
Std. Dev.:	2

50 km

Fig. 32

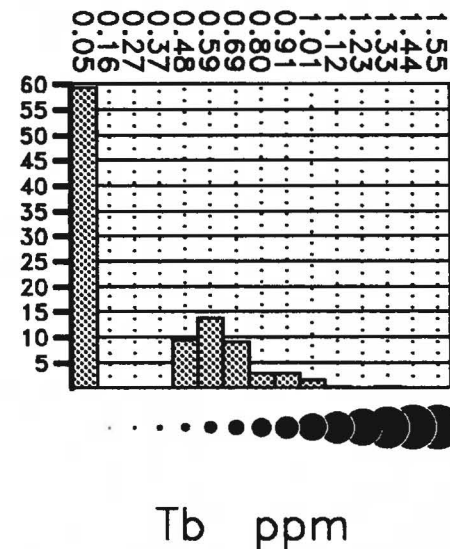
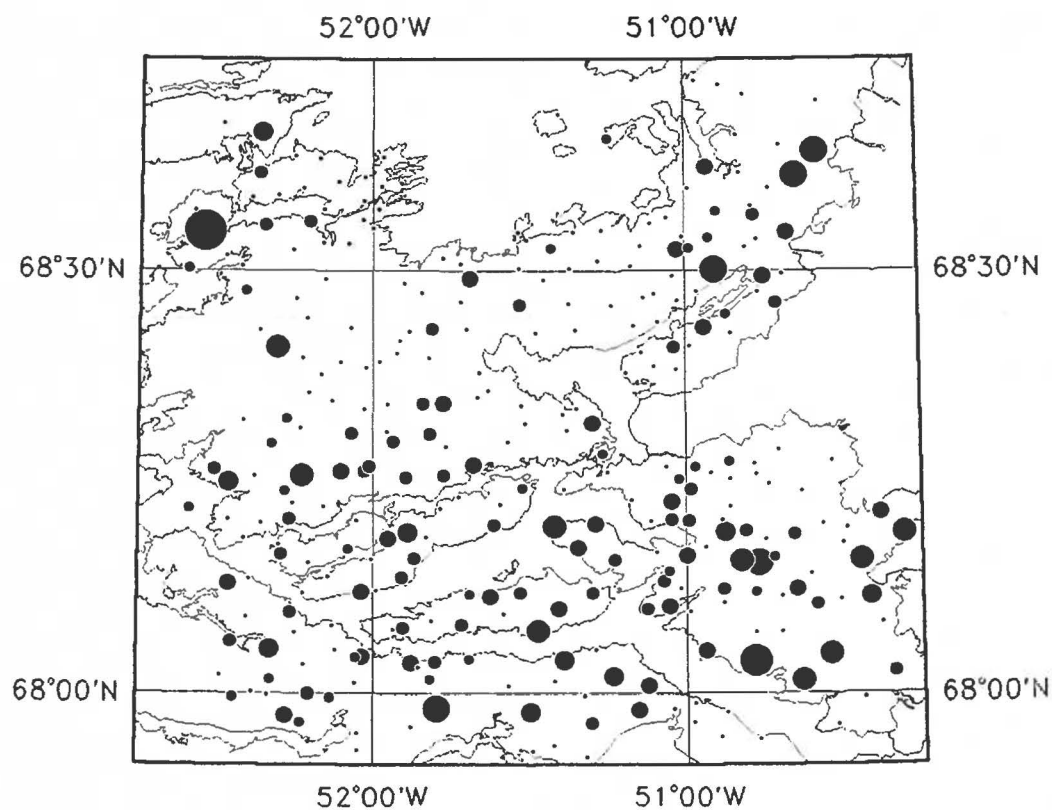


Instrumental Neutron Activation Analysis

Number of samples:	305
Min. value:	0.00
Max. value:	3.00
Mean:	1.09
Median:	1.10
Variance:	0.09
Std. Dev.:	0.30



Fig. 33



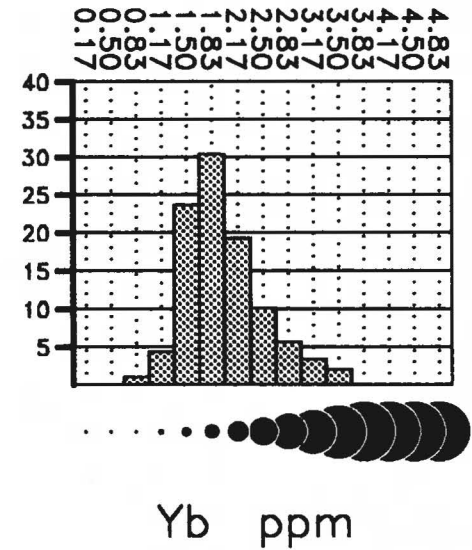
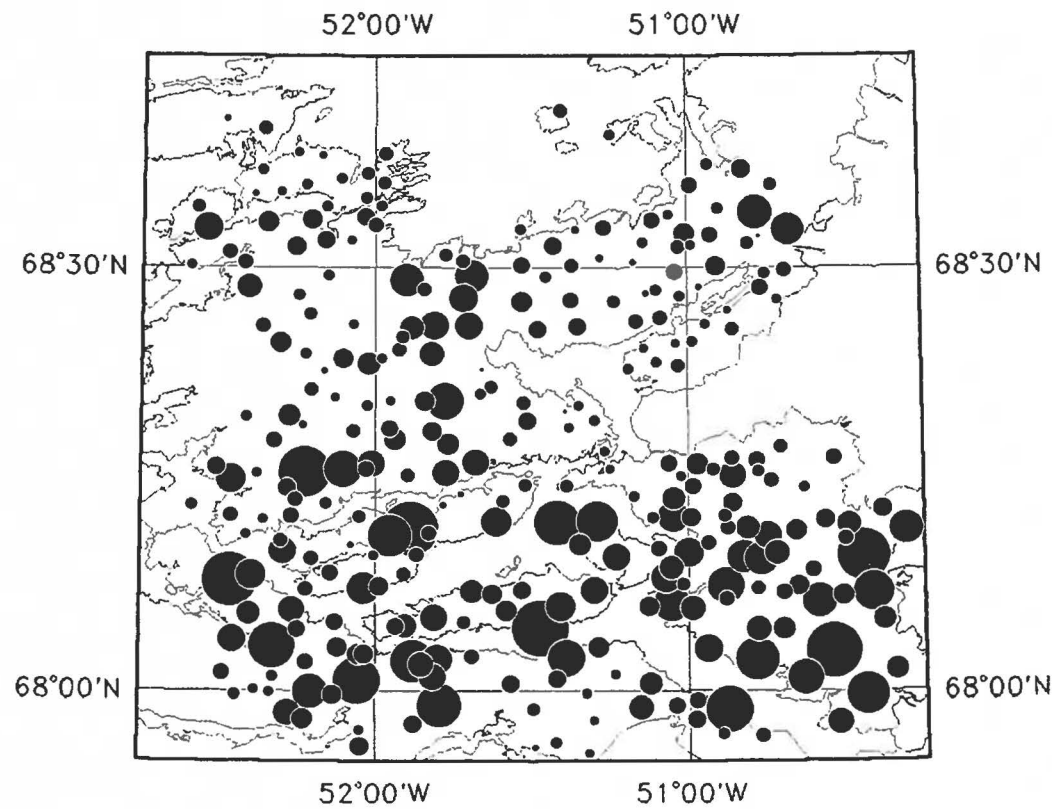
Instrumental Neutron Activation Analysis

Number of samples:	305
Min. value:	0.00
Max. value:	1.30
Mean:	0.27
Median:	0.00
Variance:	0.12
Std. Dev.:	0.34

50 km



Fig. 34



Instrumental Neutron Activation Analysis

Number of samples:	296
Min. value:	0.90
Max. value:	3.57
Mean:	1.98
Median:	1.87
Variance:	0.26
Std. Dev.:	0.51

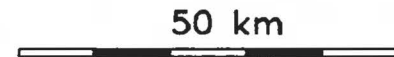
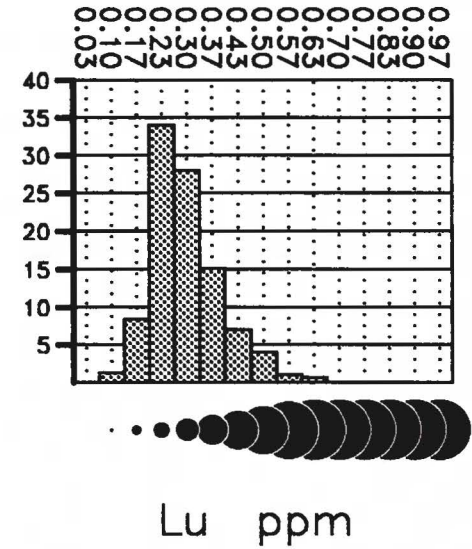
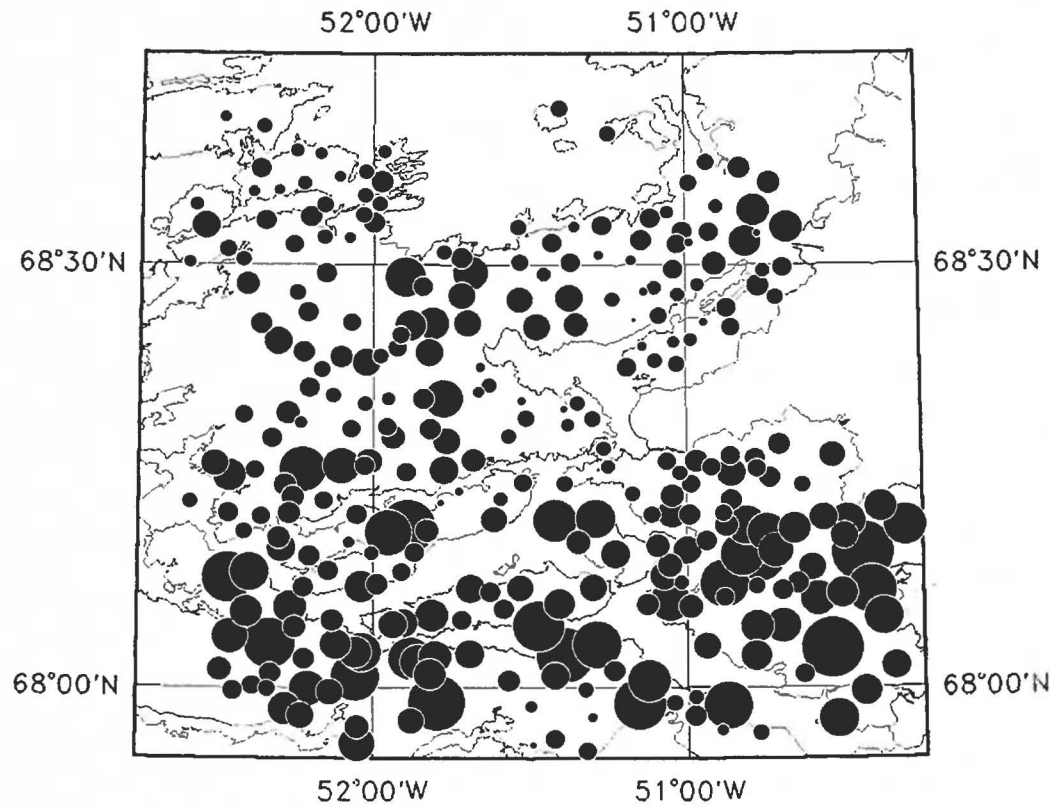


Fig. 35

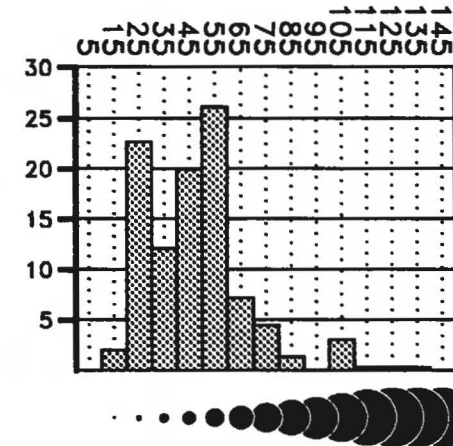
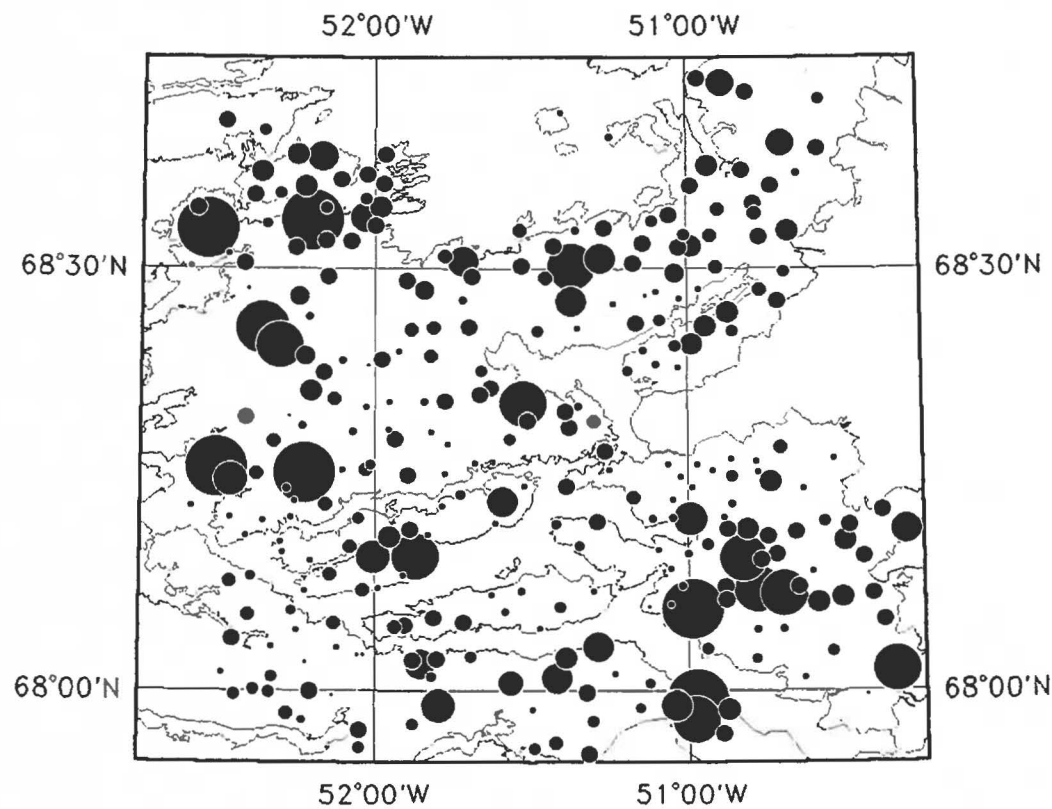


Instrumental Neutron Activation Analysis

Number of samples:	296
Min. value:	0.10
Max. value:	0.63
Mean:	0.29
Median:	0.27
Variance:	0.01
Std. Dev.:	0.09



Fig. 36



Counts per sec.

Scintillometry

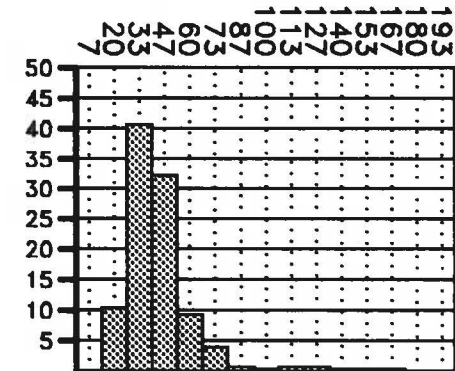
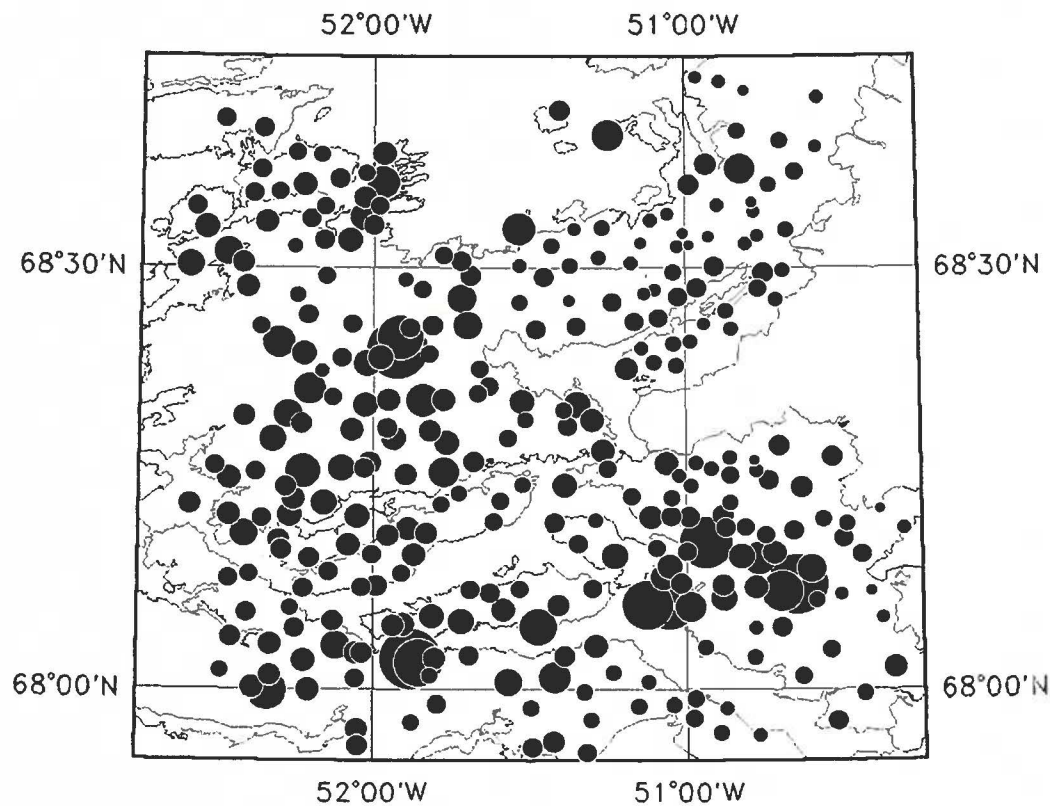
Number of samples:	295
Min. value:	10
Max. value:	550
Mean:	48
Median:	45
Variance:	1431
Std. Dev.:	38

50 km



Fig. 37

GEOCHEMICAL MAP: Conductivity of stream water



Micro Sievert

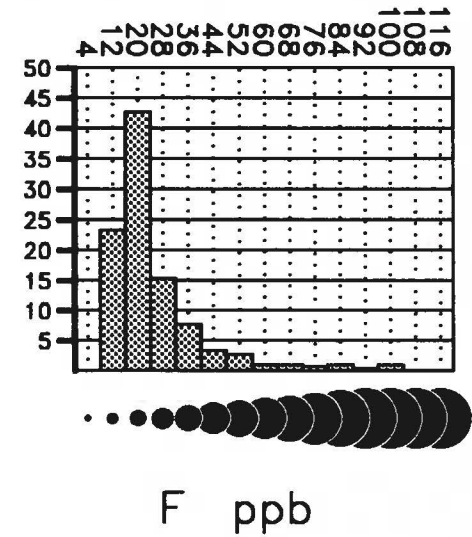
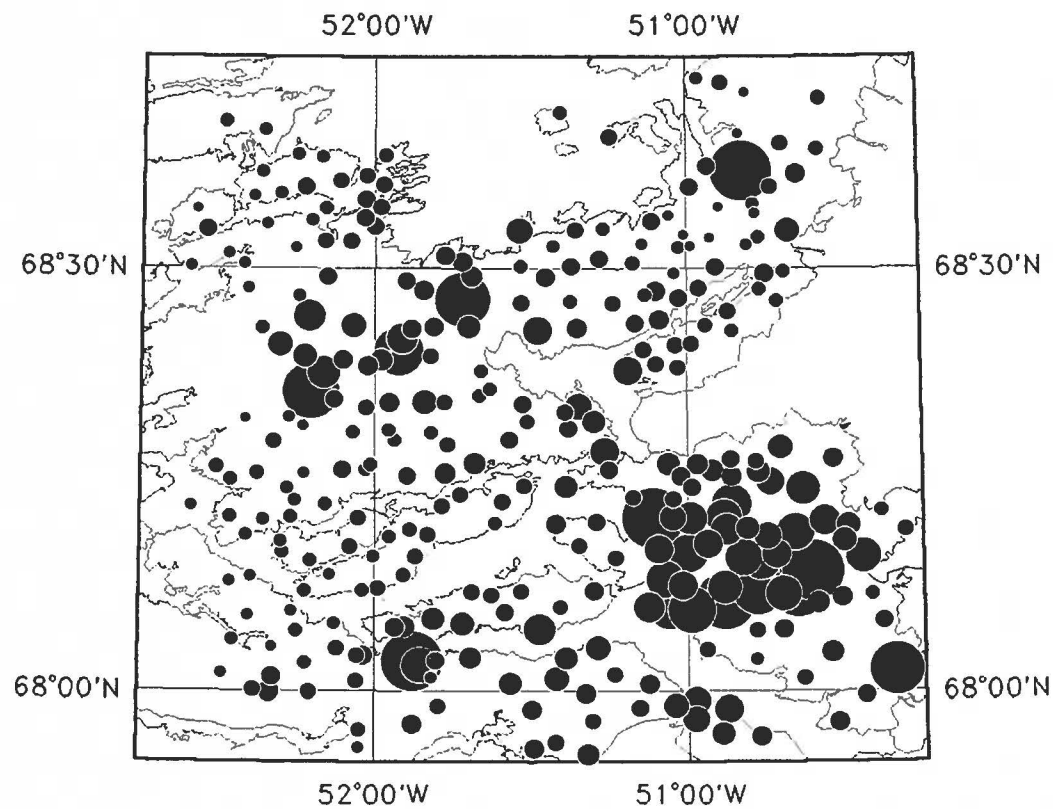
Number of samples:	301
Min. value:	15
Max. value:	323
Mean:	44
Median:	39
Variance:	628
Std. Dev.:	25

50 km



Fig. 38

GEOCHEMICAL MAP: F in stream water



Ion sensitive electrode

Number of samples:	301
Min. value:	9
Max. value:	240
Mean:	26
Median:	20
Variance:	393
Std. Dev.:	20



Fig. 39

Sketch map of "Finger Lake" prospect, Lersletten,
with location of soil samples

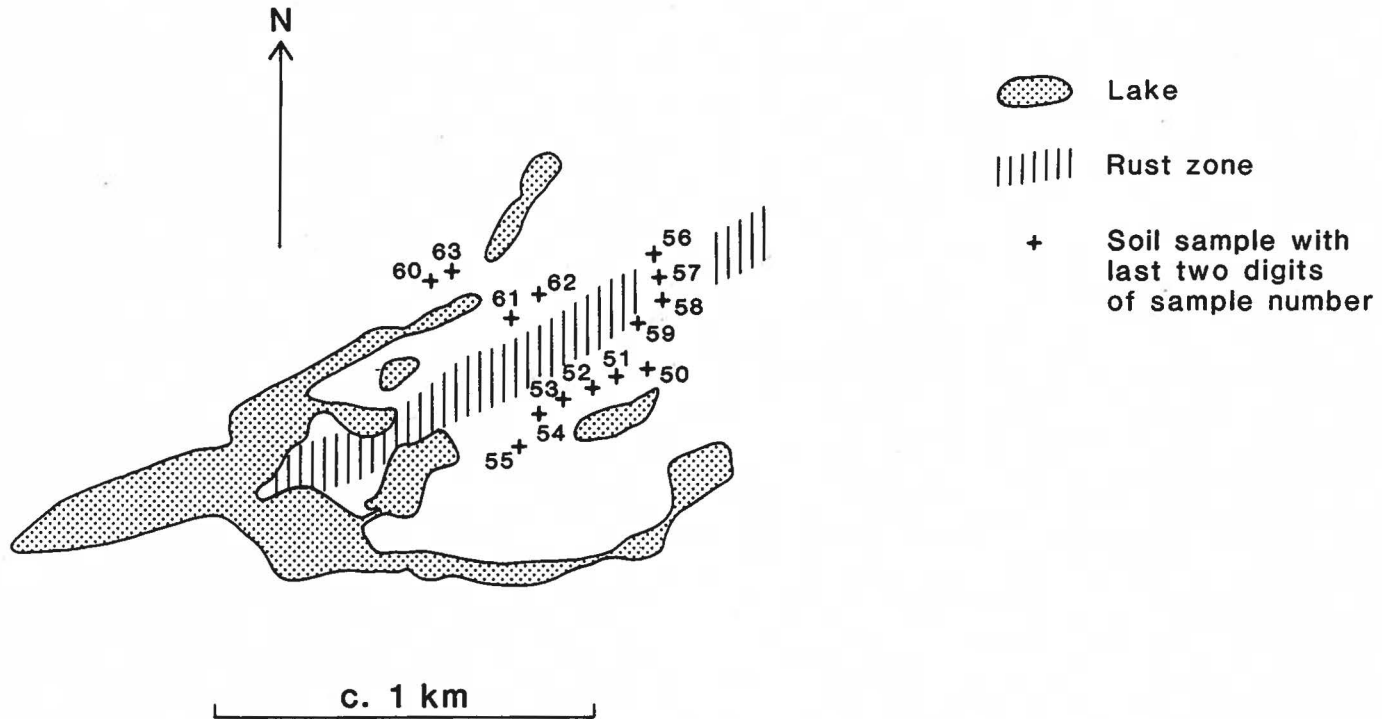
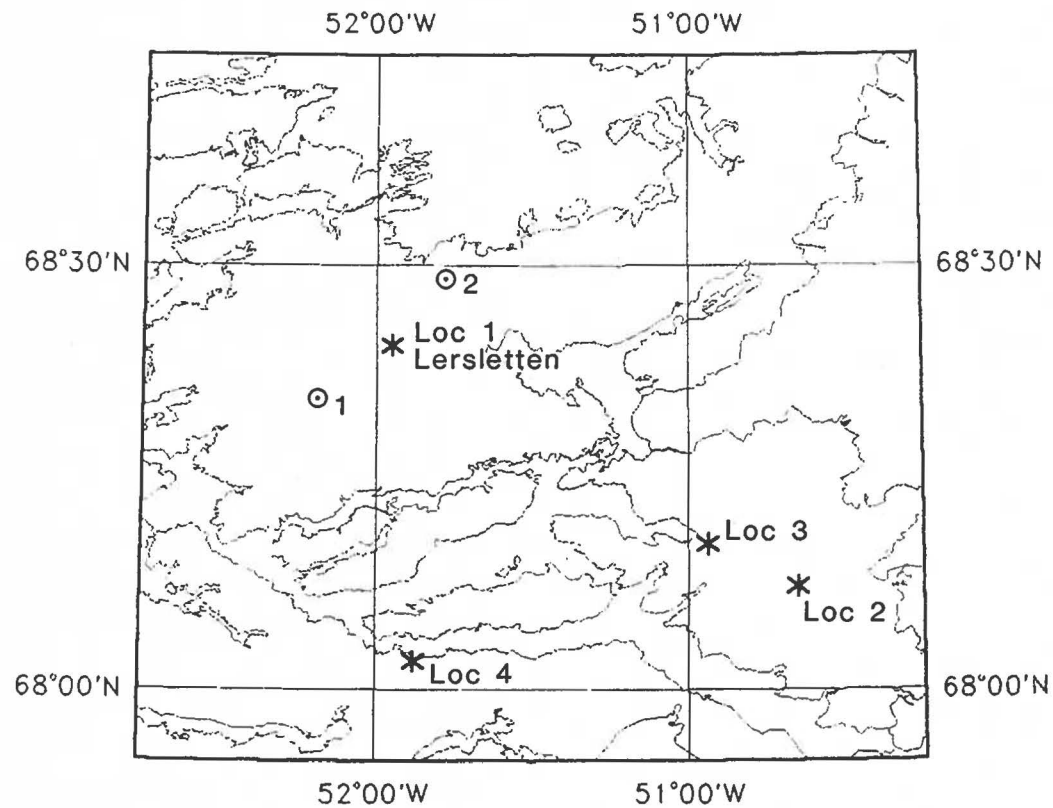


Fig. 40

LOCALITY MAP: Analysed soil, rock and clay samples



Rock samples

- * Loc 1: 360807,811
- * Loc 2: 360820,821
- * Loc 3: 360824,825,826
- * Loc 4: 360827,828,830

Clay samples

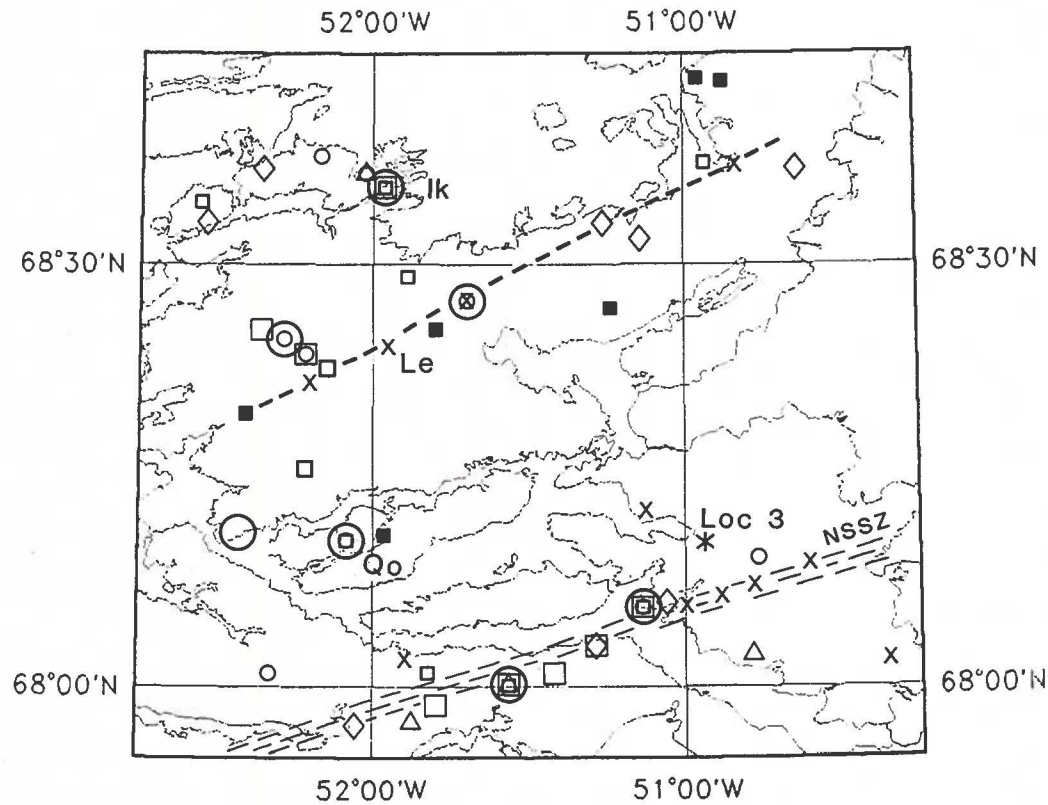
- ⊙ 1: 380152,153
- ⊙ 2: 380289,290

50 km



Fig. 41

Geochemical anomaly map



- | | | | |
|------|------------------------------|-----------------------------|-----|
| ■ | Au | > 16 | ppb |
| □ | As | ≥ 8 | ppm |
| ▣ | Sb | ≥ 0.3 | ppm |
| △ | Ba | > 600 | ppm |
| ○ | Cu | > 90 | ppm |
| ○ | Zn | > 70 | ppm |
| ◇ | U | > 20 | ppm |
| x | F (water) | > 60 | ppb |
| * | Loc 3 | Rock sample with 269 ppb Au | |
| Ik | Ikamiut | | |
| Le | Lersletten | | |
| Qo | Qoorsunnitsoq | | |
| NSSZ | Nordre Strømfjord shear zone | | |
| --- | Regional structural trend | | |

50 km



Fig. 42

